Moisture Effects on Properties of Polymeric Composite Laminates with Different Void Content

Afshin Bayatpour

A Thesis

In

The Department Of

Mechanical, Industrial & Aerospace Engineering

Presented in Partial Fulfillment of the Requirements
For the Degree of
Master of Applied Science (Mechanical Engineering) at
Concordia University
Montréal, Québec, Canada

April 2019

CONCORDIA UNIVERSITY

School of Graduate Studies

This is to certify that the thesis prepared

By: **Afshin Bayatpour**

Entitled: **Moisture Effects on Properties of Polymeric Composite Laminates with Different Void Content**

and submitted in partial fulfillment of the requirements for the degree of

Master of Applied Science (Aerospace & Mechanical Engineering)

complies with the regulations of this University and meets the accepted standards with respect to originality and quality.

Signed by the Final Examining Committee:

Dr. Chevy Chen Chair

Dr. Hua Ge External Examiner (BCEE)

Dr. Farjad Shadmehri MIE Examiner

Dr. Mehdi Hojjati Supervisor

Approved By

Chair of Department or Graduate Program Director

Dean,

Date April 15th , 2019

Abstract

Moisture Effects on Properties of Polymeric Composite Laminates with Different Void Content

Afshin Bayatpour

Composite materials, especially carbon fiber reinforced polymers (CFRPs), have been broadly used due to their high specific strength and stiffness ratio compared to metallic materials in the past few decades. CFRPs are widely utilized in aerospace, civil infrastructure and marine sectors under harsh environments. As a result, there exists a strong demand to observe the mechanical behavior of composite materials in the presence of moisture in order to avoid unpredictable effects. Composite structures are often cured in an autoclave to achieve the required aerospace grade quality. However, curing large structures requires access to large autoclaves which is limited and expensive. As a result, fabrication of large structures using out-of-autoclave prepreg materials will lead to a great amount of savings in manufacturing costs. In the out-of-autoclave processing method, the presence of voids inside the laminate has been an issue due to the lack of high pressure during manufacturing. This study aims primarily to observe the moisture absorption response of composite samples containing different levels of void. By changing the vacuum level inside the bag during the manufacturing process, three different unidirectional laminates at three levels of void have been manufactured. After immersing the samples in warm water at 60˚C for about one year, the maximum moisture absorption level and rate of absorption were monitored through experiments and diffusion coefficients were calculated for all the samples using Fick's law. Results show that the moisture absorption coefficient, its rate and the maximum level of moisture can be correlated to the void volume fraction. Moreover, the sensibility of the CFRPs under moisturized environment has been investigated. The mechanical behavior of these laminates has been studied at four different moisture levels by performing dynamic mechanical analysis (DMA) and interlaminar shear strength (ILSS) tests. Empirical results indicate that in most of the cases, interlaminar shear strength, glass transition temperature, and storage modulus decrease during the exposure of the samples with different void contents to the moisture environment. Finally, a finite element analysis has been done to study the change of moisture concentration through the thickness of the material.

Key words: out-of-autoclave manufacturing, moisture absorption, polymeric composite materials, void content, mechanical properties

Acknowledgment

I wish to express my deep and sincere gratitude and appreciation to my supervisor, Prof. Hojjati, who has been a great support to me throughout my studies and working under his supervision has been, indeed, an asset to my career path.

I also take this opportunity to acknowledge Dr. Daniel Rosca and Mr. Heng Wang who have patiently supported and guided me during the lab works. My special thanks to my colleagues in Concordia Center for Composites (CONCOM) whom I was honored to work with in such a warm and professional environment.

I would also like to thank my lovely family – Mohsen, Afsaneh, Fahimeh, and Amin - who have been and are the most precious assets of my life; they have always been the greatest support and source of energy to me and I am deeply delighted to have them by my side through all of the stages of my life.

Finally, I acknowledge my friends, on the top Amirali and Saeid, for providing me with continuous support and encouragement during my studies.

Table of Contents

List of Figures

List of Tables

Chapter 1

1 Introduction

1.1 An overview of composite materials

Fiber reinforced composite materials have achieved popularity in the industry to produce high performance products in last few decades. These days, composite materials are used in different high tech industries such as aerospace, marine, automotive and even civil infrastructures. This is because of numerous attractive advantages of using composite material like high strength and stiffness, good corrosion resistance, low coefficient of thermal expansion (CTE) and beyond that, being light weight compare to alloy and metallic parts. Being light weight can lead to huge amount of cost reduction due to the fact that reducing 1 kg of the weight of an aircraft can have a result in saving almost 3000 liters of fuel each year [1, 2]. Figure 1-1 indicates some applications of composite materials in marine and aerospace industry.

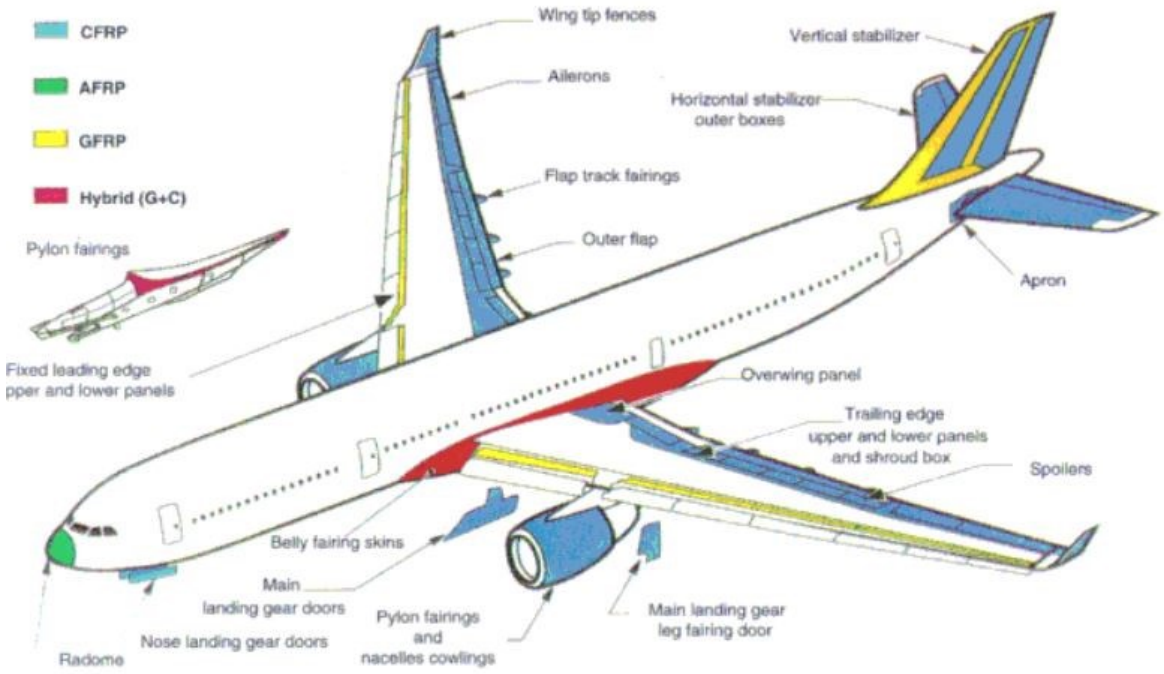

Figure 1-1 Airbus A380 structure and a business boat manufactured by composite material[3, 4]

1.2 Environment effects on composite materials

Mechanical properties of composite materials are very sensitive to the environmental conditions such as temperature, humidity, corrosive environments and etc. These environmental conditions can affect the matrix and matrix-fiber interface properties. To estimate the durability of the material which is used in the exposure of these environments, it is necessary to study the mechanical properties of them in harsh environments under different loading conditions.

Application of composite materials is increasing day by day due to their attractive advantages. It is clear that most of the composite material applications are in exposure to harsh environments such as wide range of temperature (-150 ˚C to + 125 ˚C), high vacuum, radiation and charged particles which are summarized in Figure 1-2 [5].

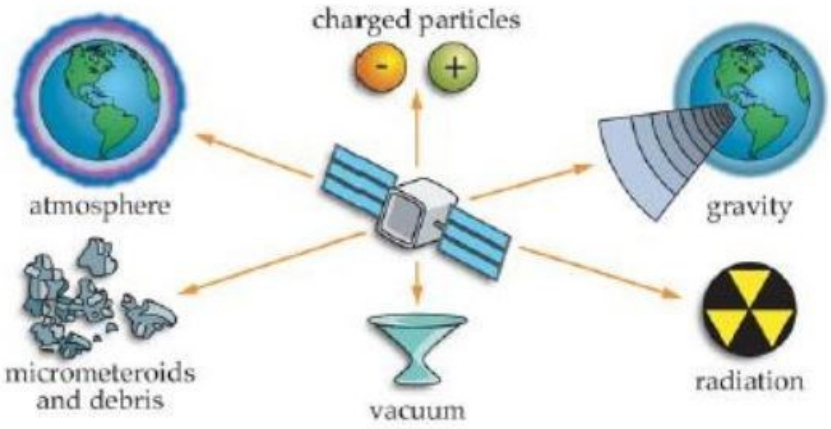

Figure 1-2 A satellite in the space in exposure of harsh environment [5].

Figure 1-3 shows the variation of atmosphere temperature and relative humidity during a day [6]. Short time or continuous exposure of the material to different moisture levels can lead to reduction in mechanical properties of composite laminates. The rudder failure of Concorde G-BOAF and the rotor collapse of a Robinson R22 Mariner helicopter VH-OHA can be considered as two major accidents made by moisture ingression into the composite structures [7-9].

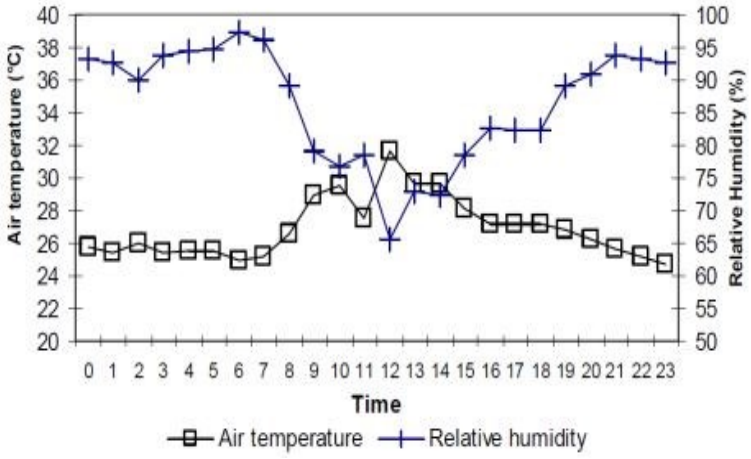

Figure 1-3 change of air temperature and relative humidity during a day [6].

1.3 Objectives of the thesis

This research aims to study the effects of moisture on properties of unidirectional carbon fiber composite materials. The main focus of our study is to investigate the moisture absorption behavior and mechanical properties of the laminates at different levels of void content exposed to the moisture. The following points, represent the objectives of our study:

- To manufacture the unidirectional laminates at different and acceptable void volume fractions using out of autoclave technique.
- To observe the moisture absorption for the CFRP laminates and study the effects of void on diffusion coefficient of the material
- To describe the effects of moisture on shear strength of the material by doing interlaminar shear strength tests at different exposure times.
- To study the moisture effects on matrix properties by investigating the viscoelastic behavior of the material and studying the stiffness of the material at different exposure times.
- To simulate the moisture absorption process, by doing finite element analysis, and comparing the results with our experimental results at all void levels.

1.4 Organisation of the thesis

The rest of the thesis includes four chapters as follows:

Chapter 2: presents a literature review on carbon fibers reinforced polymeric composites and includes the moisture absorption process in the composite materials and the affecting factors on the process. After introducing the Fickian moisture diffusion model, Chapter 2 provides the reported effects of moisture on mechanical behaviour of composites.

Chapter 3: provides the material selection process and the manufacturing protocol of the required composite laminates using out-of-autoclave procedure. It also presents the mechanical tests employed to observe the moisture effects on mechanical properties of composite laminates.

Chapter4: provides mainly the effects of moisture absorption on mechanical properties of the CFRPs and also a correlation between the sample's void content and the moisture diffusivity. A finite element analysis is done to model the moisture absorption process at micro and macro levels.

Chapter 5: presents a conclusion for all mechanical tests in the thesis and some suggestions for further research.

Chapter 2

2 Literature Review

2.1 Moisture penetration in polymers

Polymer matrix composites, especially carbon fiber reinforced polymers (CFRP) have become attractive in the last decades in various industries due to their excellent mechanical properties to density ratio. To study the effect of moisture on composite materials, it is essential to have a look at chemical reactions between the material and water molecules to know how moisture diffuses through the laminate.

Due to the fact that moisture cannot penetrate through the fibers, resin properties become very critical by affecting the function of moisture diffusion [10]. There are two factors which affect the diffusion of penetrant molecules into polymeric material: a) availability of molecular size holes between polymer chains and b) bonding forces between penetrant molecules and polymer [11], [12]. Availability of molecular size holes depends on various resin characteristics such as polymer microstructure, crosslink density, stoichiometry, and cohesive energy density while the chemical nature of penetrant molecules and polymer determine the essential bonding force between them. As a matter of fact, as the hydrogen bonding sites in polymer chains increase, the attraction between water molecules and polymer increases [13].

In this case, hydrogen bonds between polar molecules of water and hydroxyl groups (-OH) of polymer chains determine the level of moisture-polymer affinity. In this process, water molecules are divided into two categories: a) unbound molecules which can move freely inside the holes and voids but do not cause any swelling in the polymer because they just fill the free volume and, b) bound molecules which refers to the molecules that adhere to the polymer chain by hydrogen bonding. Moreover, bound molecules are the ones which cause swelling and plasticisation in the polymers, unlike the unbound molecules [12], [14].

2.2 Effective factors in moisture movement in polymeric material

a) *Nature of polymers*

Movement of a penetrant through the polymer can be different in each polymer because the nature of polymer plays a critical role in moisture transport. The amount of free volume and segmental mobility in the polymer are the factors which affect the diffusion directly. There are some other factors like degree of unsaturation, degree of crosslinking and degree of crystallinity which can affect diffusion indirectly by changing the segment mobility. Moreover, glass transition temperature has a significant influence on moisture diffusion. As T_g reduces in polymers, segment mobility and moisture diffusivity increase. Furthermore as molecular size of polymers increases, segment mobility of the molecular chains decreases drastically which leads to lower diffusion rate and moisture content [15], [9].

b) Nature of crosslinks

In the case of similarity in the nature of polymers and the crosslink density, the nature of the crosslink can affect the diffusion procedure. It is shown that as molecular chain flexibility increases, the maximum level of moisture uptake and diffusion rate increase [15].

c) Effect of plasticisers

Increasing the plasticisers in polymer chains can enhance the rubbery properties and increase the segment mobility of polymer, which can lead to a jump in diffusion coefficient and reduces the solubility of the polymer [15].

d) Nature of penetrant

Molecular shape and size is another factor that can affect the rate of diffusion in the polymeric matrix. Several studies thus far have linked the size of penetrant with diffusivity in polymers. It has been reported that as the size of penetrant molecules increases, the rate of diffusion decreases [16], [17].

e) Reinforcement

The nature of reinforcement, its compatibility with the polymer matrix and also its adhesion properties are the dominant factors in diffusion of a penetrant in filled polymers [15]. When a filler is not compatible with the matrix nature, the amount of void content increases at the interface, which can increase the free volume and also the rate of diffusion. On the other hand, in the case of compatibility of the reinforcement and the polymer system, the filler can go through the void contents and reduce the diffusivity [18]. Moreover, using the fillers can reduce and restrict the mobility of the penetrant, which can again lead to reduction in diffusivity [19], [20].

The difference in the coefficient of thermal expansion (CTE) and the coefficient of moisture expansion (CME) between the fibers and the matrix can make the swelling an anisotropic phenomena in composite materials. Swelling decreases by increasing the fiber volume fraction and can be negligible in the presence of a strong interface [21], [22].

f) Temperature

In most cases, increase in temperature leads to decrease in solubility and increase in both diffusivity and maximum moisture content in the composite materials [23]. Gillat et al, studied the moisture diffusion of T300 graphite/epoxy under different external loadings at 25 ˚C, 60 ˚C and 80 ˚C for two different cross-ply laminates. They observed an increase in diffusivity and maximum moisture content as immersion temperature increased [24]. Lv et al, discovered that an increase in diffusivity at a higher immersion temperature is due to an increase in molecular chain relaxation and reduction in T_g and molecular bonding strength at higher temperatures [25].

2.3 Describing moisture diffusion by Fick's law

Fickian diffusion is the most common diffusion model for modeling the moisture absorption procedure through polymeric material. This model was described by Adolf Fick in 1855 for steady state (Fick's first law) and non-steady state (Fick's second law) diffusions [26]. The driving force which leads to the molecular transportation is difference in concentration, which moves the penetrant molecules from higher concentration areas to lower concentration areas in the solvent. This movement ends when the polymer reaches the equilibrium mass concentration.

This phenomena is described by Fick's first law of diffusion and relates diffusion flux to the concentration gradient as:

$$J = -D\left(\frac{\partial c}{\partial x}\right) \quad (1)$$

Where

J is the diffusion flux $[\frac{g}{mm^{-2}s^{-1}}]$

D is coefficient of diffusion or diffusivity $[mm^2s^{-1}]$

c is mass concentration $[\frac{g}{mm^{-3}}]$

Fick's second law explains the moisture diffusion when concentration gradient changes as time goes on. In our study, we considered one-dimensional diffusion. The following equation is Fick's second law of diffusion with assuming the constant diffusivity.

$$\frac{\partial c}{\partial t} = D_x\left(\frac{\partial^2 c}{\partial x^2}\right) \quad (2)$$

Where

c is the moisture concentration $[\frac{g}{mm^{-3}}]$

D_x is the coefficient of diffusion through the thickness of laminate $[mm^2s^{-1}]$

x is the distance in the direction of thickness [mm]

t is time [s]

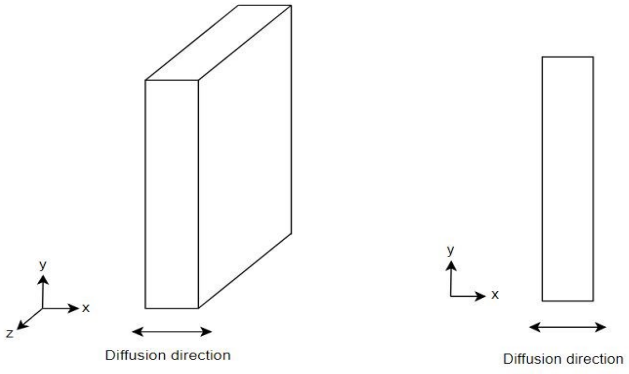

Figure 2-1 3D and 2D view of moisture absorption process

Figure 2-1 shows the moisture diffusion through the thickness of the material in 3D and 2D views. In this study it is assumed that moisture penetrate along x direction in the figure above.

For the infinite plate (width and length >> thickness), only the surfaces which are exposed to the moisture will reach and remain at the maximum concentration equilibrium very fast. In other words, the boundary conditions are as follows:

$$c = c_i \qquad 0 < x < h \qquad t \leq 0$$
$$c = c_m \qquad x = 0, x = h \qquad t > 0$$

Where

c_i is the initial moisture concentration (in our case it is zero)

c_m is the maximum moisture concentration

h is thickness of the sample

t is the exposure time

To solve the equation 2, Jost suggested the following solution considering the above boundary conditions [27]:

$$\frac{c - c_i}{c - c_m} = 1 - \frac{4}{\pi}\sum_{j=0}^{\infty}\frac{1}{(2j+1)}\sin\frac{(2j+1)\pi x}{h}\exp\left(-\frac{(2j+1)^2\pi^2 D_x t}{h^2}\right) \qquad (3)$$

A schematic of perfectly Fickian moisture absorption process is described by Figure 2-2. After finishing the absorption process, when the laminate reaches its maximum level of moisture content, considering the initial linear slope of the absorption curve, the diffusion coefficient of the material can be described as follows[28]:

$$D_x = \pi\left(\frac{h}{4M_m}\right)^2\left(\frac{M_2 - M_1}{\sqrt{t_2} - \sqrt{t_1}}\right)^2 \qquad (4)$$

Where

h is thickness of the sample [mm]

M_m is the maximum level of absorbed moisture [g]

M_2 and M_1 are two points in the linear region, for calculation of the initial slope of the curve

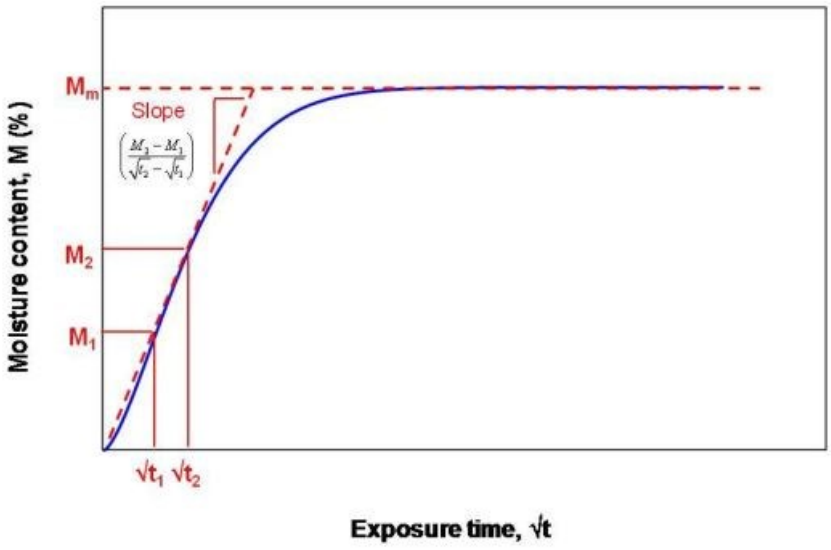

Figure 2-2 a moisture absorption process which perfectly follows Fick's law[9].

2.4 Out of autoclave manufacturing

Manufacturing method is one of the most dominant factors in composite material properties. Although nowadays composite structures are mostly cured in autoclave to reach space grade level, autoclave has its own disadvantages. Using autoclave increases the cost of the process itself, while curing large structures requires bigger autoclaves, which can further increase the cost of the manufacturing process. Out of autoclave (OOA) technique is an alternative which can reduce the cost of manufacturing and speed up the process. Figure 2-3 indicates the schematic of both techniques [29].

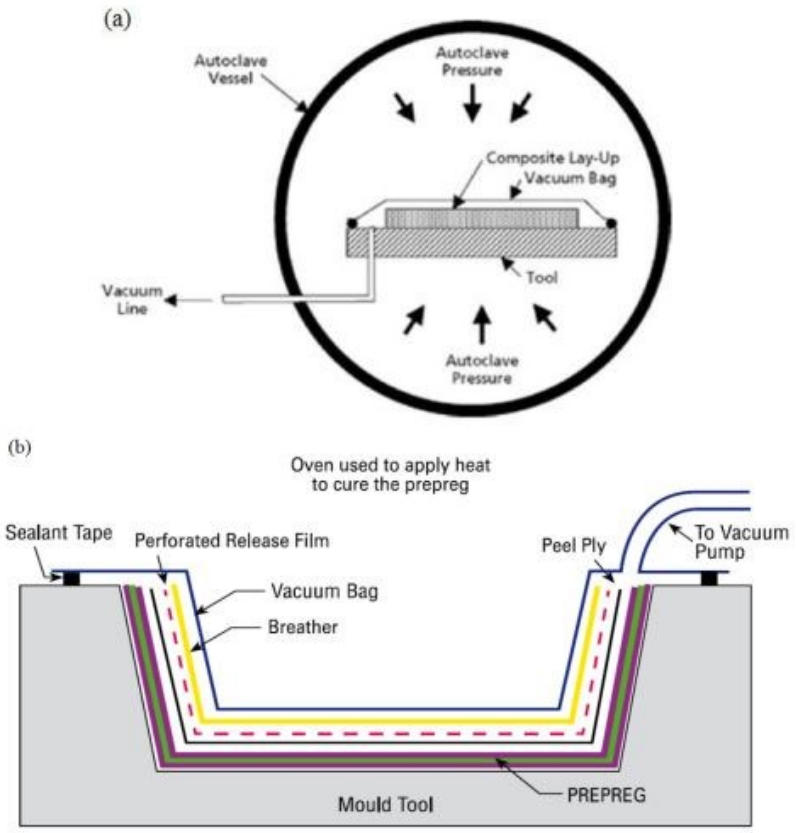

Figure 2-3 manufacturing the composite laminate using a) autoclave and b) out-of-autoclave techniques [29].

In last few decades, OOA material prepregs have become more acceptable in industrial manufacturing due to the same quality as autoclave manufactured samples, using vacuum bag pressure only (VBO). In OOA, required pressure has been achieved by applying a vacuum pump to minimize the void in the laminate. Since we cannot provide high pressure using vacuum bags, we expect to have more void content using OOA technique [30]. There are some small ovens with the capability of connecting vacuum pumps during the manufacturing process, which can maintain the required temperature and pressure with much lower cost compare to expensive autoclaves.

There have been a lot of investigations comparing these two techniques. Caroline Dang et al. [31] examined mechanical properties such as short beam shear strength, combined loading compression, open hole compression, tension and flange bending specimens which resulted in comparable outcomes to the IM7/8552 data sheet. Centea et al. [32] reported that desired quality in OOA is dependent on some factors including the properties of the fibers and resin, the original

state of the prepreg, cure parameters such as temperature, vacuum quality, and part characteristics like geometric complexity and size. They also mentioned by reducing the consumed energy in the curing process at OOA, they had a 6 percent reduction in costs compared to the autoclave technique. Sutter et al. [33] compared these two techniques in manufacturing of a heavy lift space launch structure. They found out prepreg out-life has a dominant effect on the sample quality. They tested two types of samples; one with less out-life time which was built right after thawing, and the other one which was made by prepregs with more out-life. Comparing the results of these groups for short beam shear strength, compression strength, and open hole compression strength, they discovered they can have a close to autoclave quality sample (higher mechanical properties and less void content) when they use fresh prepregs.

Based on this study, having more void content and thickness deviation are two difficulties which we may face during OOA process.

2.5 Environmental effects on mechanical behaviour of composite materials

Since mechanical properties play a critical role in composite material performance, there have been a lot of investigations to measure the changes in mechanical behaviour when they are exposed to harsh environments. Nowadays there are a lot of applications for composite materials used in high moisture level environments. Therefore studying mechanical properties in such situations have become the main focus among researchers and designers. Generally it has been reported that the matrix is the main part of composite laminate which can be affected in harsh environments. Mechanical properties of the laminates, such as modulus and strength, can change with moisture absorption. It has been reported that exposure to the moisture environment can lead to increase in flexibility and ductility while it can reduce the elastic modulus and strength [34], [35]. In this literature, our main focus is to study strength and stiffness of composite laminates. Hence, we have investigated how the mechanical properties of composite materials change after moisturising.

2.5.1 Inter laminar shear strength (ILSS)

Inter laminar shear strength is one of the most important mechanical tests to measure shear strength of matrix layers between adjacent layers. Three point bending of a short beam is one of most common fixtures for determining ILSS to discover matrix dominant properties [36]. A typical setup for flat samples is provided below. To achieve valid results, the following geometries are suggested:

$$\text{Speciment length} = \text{Thickness} \times 6$$

$$\text{Speciment width} = \text{Thickness} \times 2$$

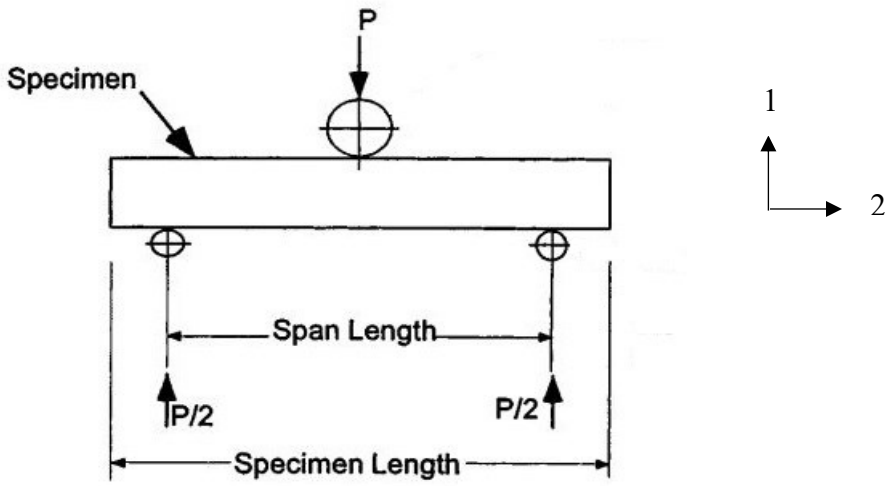

Figure 2-4 A typical test configuration for measuring the short-beam strength based on ASTM standard [37].

To determine the shear strength of a unidirectional laminate, samples are cut as the fibers are parallel to the length of the samples (direction 2 in Figure 2-4). Based on the classical beam theory, it has been shown that maximum normal stress caused by bending occurs on top or bottom layers (compressive stress and tensile stress relatively). Considering the small amount of span length to thickness ratio (l/h), we can neglect maximum stresses in outer layers resulting from bending moment compared to shear stress in the mid-plane [36]. Based on ASTM D 2344, the minimum acceptable thickness for this test is 2 millimetres. Also, the span length-to-specimen thickness ratio should be fixed at 4.

Shear strength in the mid-plane is calculated by following equation:

$$\tau_{ILSS} = 0.75 \times \frac{P_m}{b \times h} \quad (5)$$

Where

τ_{ILSS}: short beam strength (MPa);

P_m: maximum load observed during the test (N)

b: measured laminate width (mm);

h: measured laminate thickness (mm) [37].

There have been numerous studies on the effects of voids and moisture on ILSS properties of composite laminates. Bowles et al. [38] studied the effects of void content on ILSS of a polyamide matrix composite. They measured the composite densities and the fiber volume contents of almost 30 laminates and made a correlation between ILSS and composite density. With the growth of void content, they saw an increase in scatter in strength data. Joshi [39] studied the effects of moisture on interlaminar shear strength of a unidirectional carbon/epoxy laminate. He moisturized the samples either by immersing them in hot water or aging in a hot and humid atmosphere. He found reduction in ILSS and their dependency in the amount of absorbed moisture not to the mode of exposure. He explained Plasticization, swelling and debonding as the main factors for shear failure.

Zike Wang et al. [40] examined ILSS for basalt, glass and carbon fiber reinforcement polymer bars (BFRP/GFRP/CFRP) immersed in sea water. They compared different methods of short shear tests and they observed the effect of span length to diameter ratio. Based on their experiences, BFRP had the greatest ILSS while GFRP had the weakest ILSS. Daniels et al. [41] carried out ILSS of unidirectional epoxy matrix composites with different types of graphite fibers. They observed a peak for strong samples and a plateau for weak specimens in short beam shear stress versus deflection curves. They also reported a strong dependency on $(\frac{L}{h})$ value for ILSS. A sudden drop in ILSS occurred around glass transition temperature according to reduction in the mechanical behavior of the matrix.

In a research work organized by Pavildou et al. [42] water absorption and reabsorption of three different types of glass fabric/polyester composite (clean fabrics, fabrics with silane, and fabrics with PDMS (Polydimethylsiloxane)) with variety in interfacial strength were studied. In dry state, silane treated samples showed much higher resistance against shear stress because silane coating improve chemical bonding at the interface. Moreover, in silane treated samples, moisture cycles did not affect ILSS while in case of PDMS and clean fabrics, moisture cycles had a higher impact on ILSS. They believed that absorbed water makes debonding much easier and that is why in presence of moisture ILSS is decreased.

Vina et al. [43] studied mechanical behaviour of PEI/Glass and PEI/carbon fiber composite samples by examining tensile and interlaminar shear strength. As it is clear in Figure 2-5, both tensile and interlaminar shear strength faced a decrease in the first 5 days of moisturising and after that they remain almost constant.

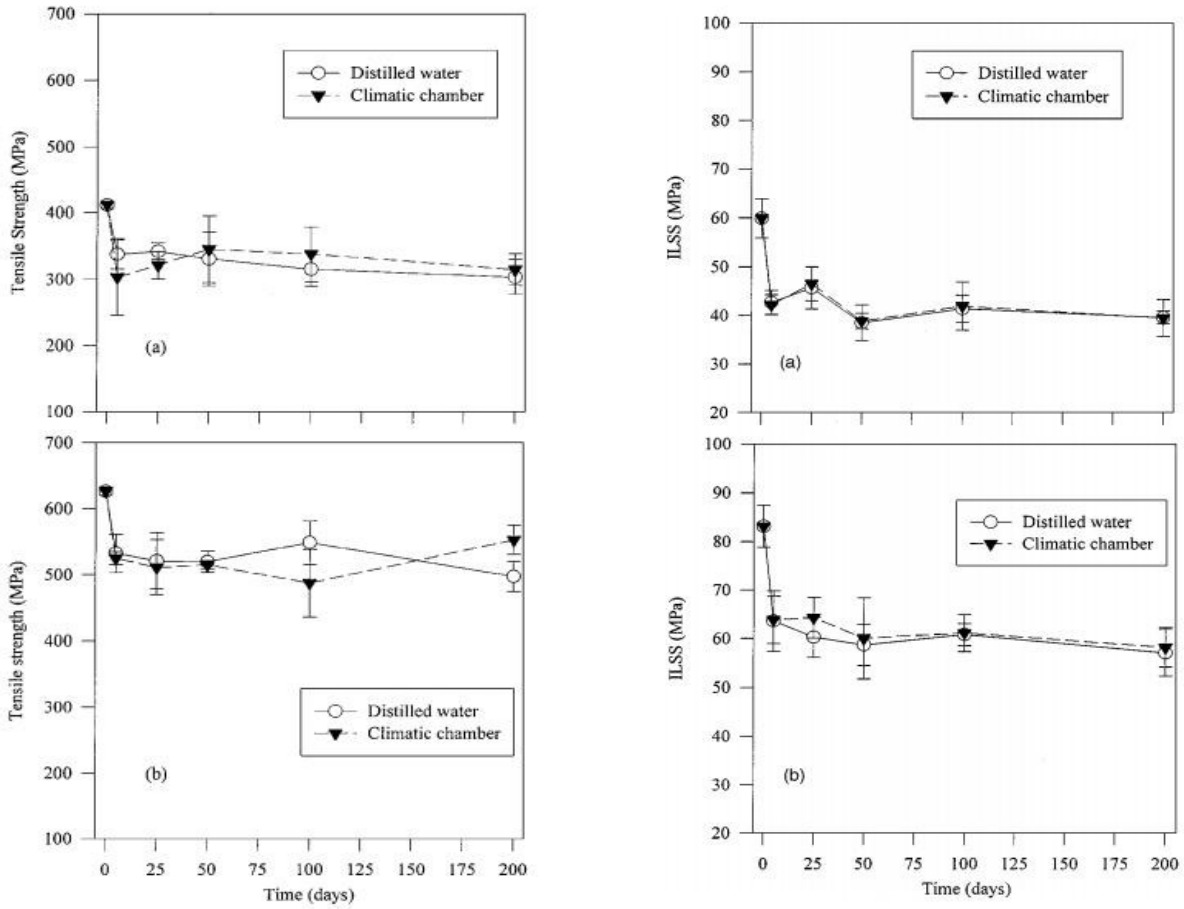

Figure 2-5 tensile strength and ILSS at different moisture levels [43].

2.5.2 Dynamic mechanical Analysis (DMA)

Doing DMA can give us a broad vision on mechanical properties of the laminate such as T_g, storage modulus, loss modulus and damping factor. T_g or glass transition temperature, is the temperature that the laminate changes from solid to the rubbery state which occurs with sharp drop in stiffness and increase in viscosity. DMA is considered one of the most sensitive analysis to any change in material properties of the material especially in polymeric materials [44, 45]. DMA has been investigated by many researchers which we will go through in the following:

Hassan et al. [46] studied the effect of moisture on mechanical behaviour of Technyl A216, and Technyl A216 V30NAT at three different levels of fiber volume fraction by doing dynamic mechanical analysis. Samples were immersed in boiling water for at least 24 hours. The damping factor of the composite material was studied at the temperature range of -100 ˚C to 150 ˚C for dry and moisturized samples and the results are shown in Figure 2-6. At the dry condition (A), two transition areas were monitored. B-transition was referred to the transition at lower temperature while the α-transition was related to the higher temperature and T_α represents the glass transition temperature. The reason for occurring pick values at lower temperatures was not clear in the literature but it was reported that it is related to the polar groups in the water-polymer complex units[47]. As it can be seen a left shift can be seen in the tan δ graph after moisturizing which can show the reduction in T_g. Several other authors [48-51] also studied the moisture absorption process on composite materials and its effect on the damping factor and the glass transition temperature of the material and they have reported the same results as Hassan.

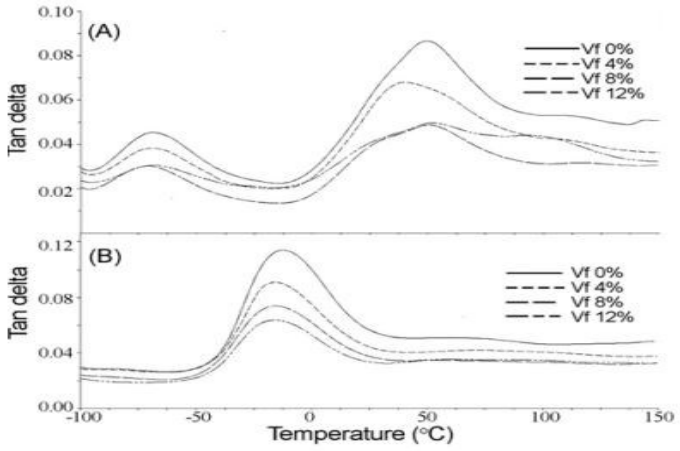

Figure 2-6 variation of Tan δ at different levels of moisture content for different fiber volume fractions at A) dry condition and B) after moisturising [46].

2.6 Conclusion

As discussed in this chapter, moisture absorption of composite laminates had been studied in last few decades in the literature. However, to the best knowledge of the author, moisture absorption of the composite laminates at different levels of void volume fractions is not studied. This research aims to contribute to the literature by studying the diffusion coefficient of the laminates in different void levels and investigating the mechanical properties of the laminates such as strength, stiffness, and glass transition temperature at dry condition and after absorbing moisture.

Chapter 3

3 Experimental Process

3.1 Material selection

In this research, CYCOM 5320-1, produced by Cytec Engineered Materials Inc. has been used which is one of the most common materials in aerospace applications especially in out of autoclave manufacturing. In this research we made unidirectional laminates using OOA procedure. Applying different vacuum levels, three different laminates with different void contents were achieved and their mechanical properties such as ILSS, glass transition temperature, storage and loss modulus were examined after exposure to the moisture. Table 3-1 material properties privided by the manufacturer [52] shows material properties of prepregs.

Table 3-1 material properties privided by the manufacturer [52]

Property	UD OOA
Manufacturer	Cytec Materials
Fiber	T650-UD carbon
Resin	Cycom 5320
Tow count (fiber/tow)	Nil
Yarn width (mm)	Nil
Areal density (g/m^2)	882.34
Resin content (%)	36

3.2 Manufacturing using Out of Autoclave technique

One of the most challenging parts of this research is the ability of producing composite laminates with different and acceptable levels of void contents. In hand lay-up process, the applied pressure to the resin and vapor pressure from the trapped moisture between the plies play a critical role in formation of voids inside the laminate. During the manufacturing process, when the applied

pressure from the vacuum bag becomes less than the vapor pressure between the plies, porosities can form [53]. To add extra void content, Costa et al [54], produced homogenous void content in the laminate by spraying water uniformly during the layup procedure and having control on applied pressure on resin. To avoid having chemical reactions between the layers, we decided to add void content to the laminate by changing the vacuum pressure in the manufacturing process.

In this section we go through the manufacturing steps of the composite laminates. Three different laminates containing 24 layers with 200 mm × 200 mm dimensions were made at different levels of void contents by applying different vacuum pressures.

3.3 Layup process

An overall overview of vacuum bag setup is presented in Figure 3-1. The hand lay-up procedure was done based on the steps which are presented below [55]:

a) Before cutting the prepregs to the desired dimension, the prepreg layers were put at room temperature for about 2 hours to have a uniform thickness with minimum waviness and good surface finishing at the final product.
b) Before putting the first prepreg on top of the mold, it is recommended to clean the surface of the mold to have the better surface finishing. After cleaning, a thin layer of release agent was used to ease the demolding process after curing. Next, prepregs were stacked up one on top of another. During stacking process, facing to trapped air is very common between the layers. A roller was used to remove the trapped air and reduce the void content with applying pressure on top of the prepregs. It needs to be mentioned that in our case, for the samples with less void content, the roller was used more often.
c) After finishing lay-up process, one thin layer of release film was applied. Then, a bleeder layer was used to absorb the extra resin during the curing process. Normally prepregs hold more resin than what will be left in the composite laminate. This extra resin will flow out and goes into the bleeder material. At the next step, a breather layer was applied which allow the moisture vapors that was forming during the curing process to escape. The last layer was the vacuum bag which covered the laminate surface. The vacuum bag

was attached to the mold edges by using sealant tapes. Vacuum bag was used to make a pressure on top of the laminate to reduce the void content and remove the volatiles and moisture during the curing.

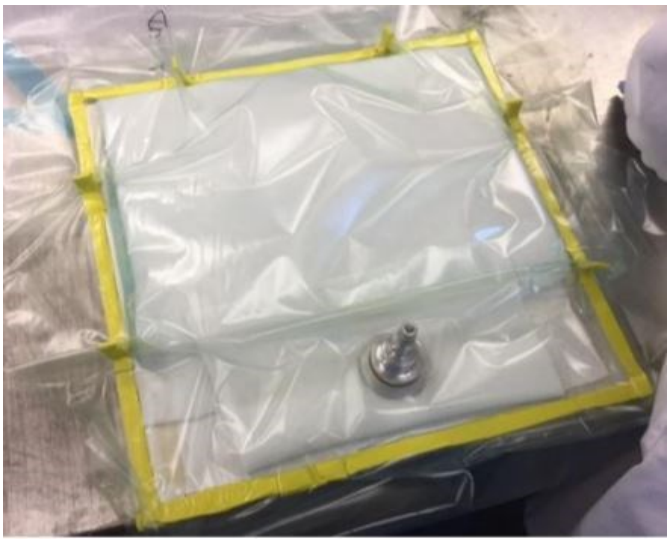

Figure 3-1 schematic of the vacuumed sample before curing

In this study, for having three levels of void contents, we changed the vacuum level and frequency of using the roller during the lay-up process. The vacuum pressure and frequency of using the roller is described below for each void level.

Table 3-2 vacuum pressure and roller usage frequency for each level of void content

Void content	Vacuum pressure (MPa)	Roller usage frequency
0.2% ± 0.05%	0.099	Every layer
1% ± 0.05%	0.067	Every 4-layer
2% ± 0.05%	0.034	Every 8-layer

3.4 Curing procedure

A curing cycle suggested by Cycom 5320-1 was followed to have perfectly cured composite laminates [56]. An especial type of forced air circulation oven was used in curing process to maintain the required pressure during the curing cycle. The required pressure was applied continuously by a vacuum pump during the process.

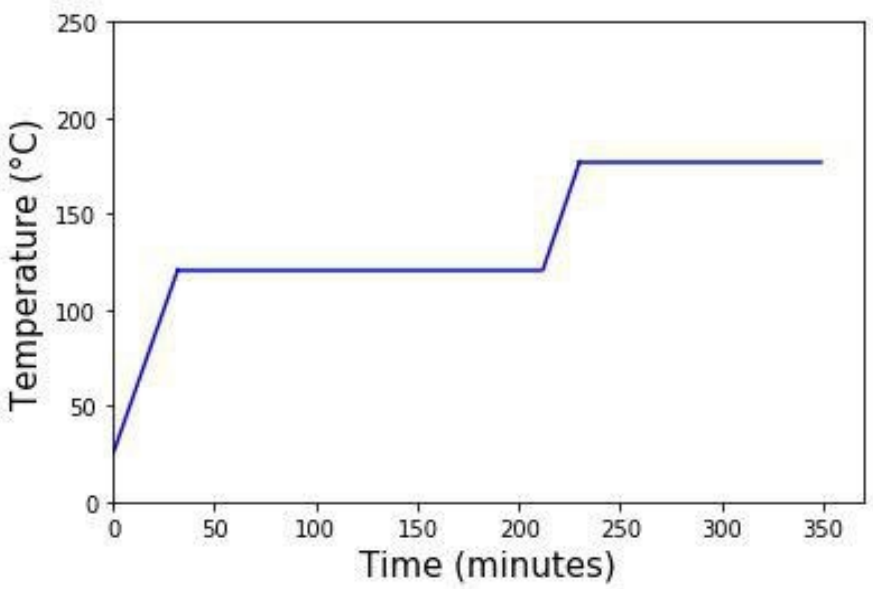

Figure 3-2 the recommended curing cycle by the manufacturer

Figure 3-2 indicates the recommended curing program for the curing cycle. As it can be seen, the oven temperature was increased from room temperature to 121 ˚C with a ramp rate of 3 ˚C/min and was held for 3 hours to complete the curing stage. Next, the temperature again was increased with the same rate to 177 ˚C and kept for 2 hours to finish the post-curing period. At this point, the temperature was allowed to cool down to the room temperature. Three different unidirectional laminates were manufactured using this technique. Figure 3-3 shows the final UD laminates.

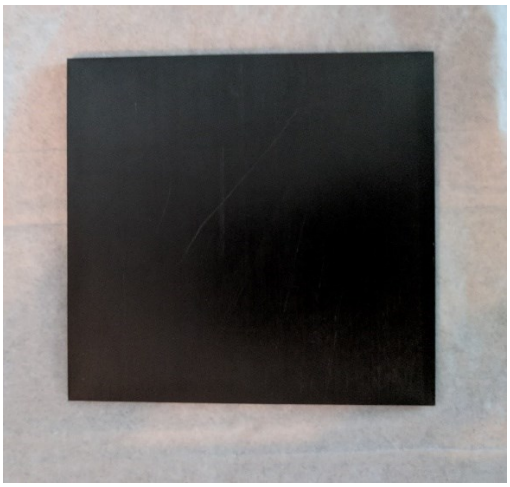

Figure 3-3 manufactured laminate after curing and demolding process

3.5 Sample preparation

Three different UD laminates having different levels of void contents have been fabricated at previous steps. To study the moisture absorption behavior and mechanical properties of laminates under harsh environment, samples were cut to required dimensions based on different standards. Before preparing samples for the tests, all four laminate edges were cut around 10mm to remove round corners from the sides. Coupon dimensions and the size guides are provided on Table 3-3 based on related standards. To cut the samples, a circular saw machine with coolant was used. The final samples for ILSS and DMA tests are shown below.

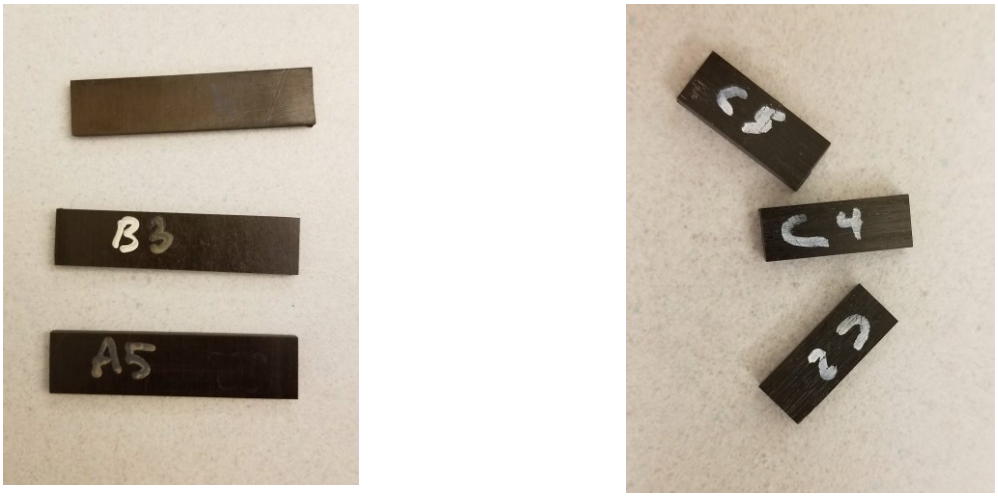

Figure 3-4 DMA and ILSS samples after cutting

Table 3-3 a summary of sample dimensions for different tests based on related standards

	Tests		
	DMA	ILSS	Moisture absorption
Sample width (mm)	10	6.5	100
Sample length (mm)	50	20	100
Number of repeats	2	3	2
Related standard	DMA manual	ASTM D2344	ASTM D5229

3.6 Void content measurement

Void content percentage had been verified by doing microscopic observation for three random specimens from each main plate. For measuring void contents, microscope's software was used which utilized difference in transparency in each cross section. To do the optical microscopy, it is required to have a great surface finishing. To measure the void content, fibers should be perpendicular to the cross section of sample. The samples were polished step by step from coarse size grinding paper to the finest size. Figure 3-5 shows the optical microscopy for all three laminates. After microscopy the amount of 0.2%, 1% and 2% void content for each laminate was observed.

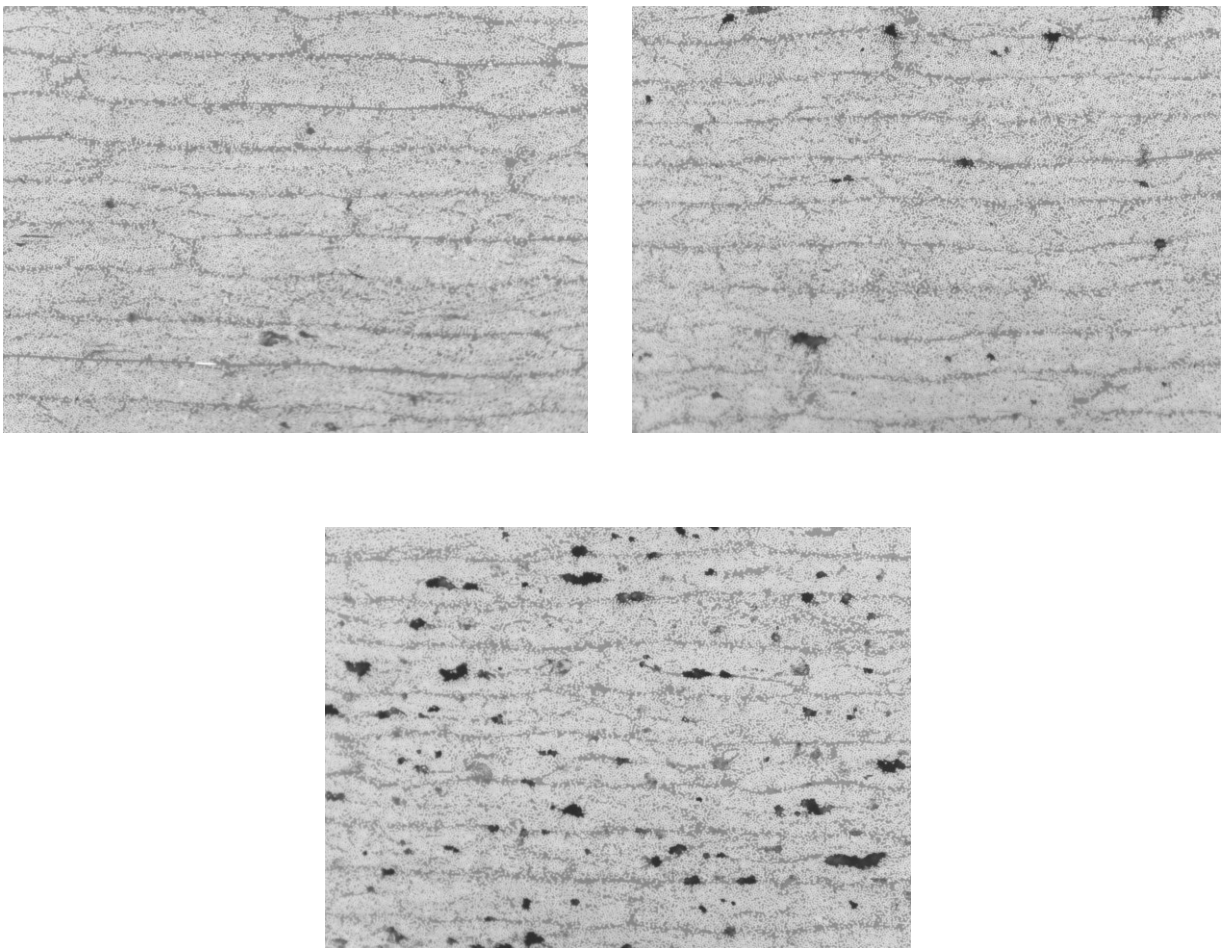

Figure 3-5 optical microscopic evaluation for the composite laminates

3.7 Moisture absorption procedure

After cutting the samples, it is crucial to dry the samples. After measuring the initial weight of the samples, we have put them in oven at least for 12 hours at 60 ˚C. During the drying procedure, we monitored the weight of samples and the procedure was stopped when the weight does not change more than 0.02% as time goes on. At this step, the last monitored weight was labeled as W_d. the primary aim of this study is to obtain the through the thickness diffusivity and moisture absorption behaviour of composite laminates. To do so, the samples were bonded by stainless steel foil at the edges. Before starting the moisturising, we monitored the weight of sample one more time to avoid having trouble in calculating the moisture absorption level due to mass increase because of the steel foil. Figure 3-6 shows the samples after adding the stainless steel foil and moisturising pot.

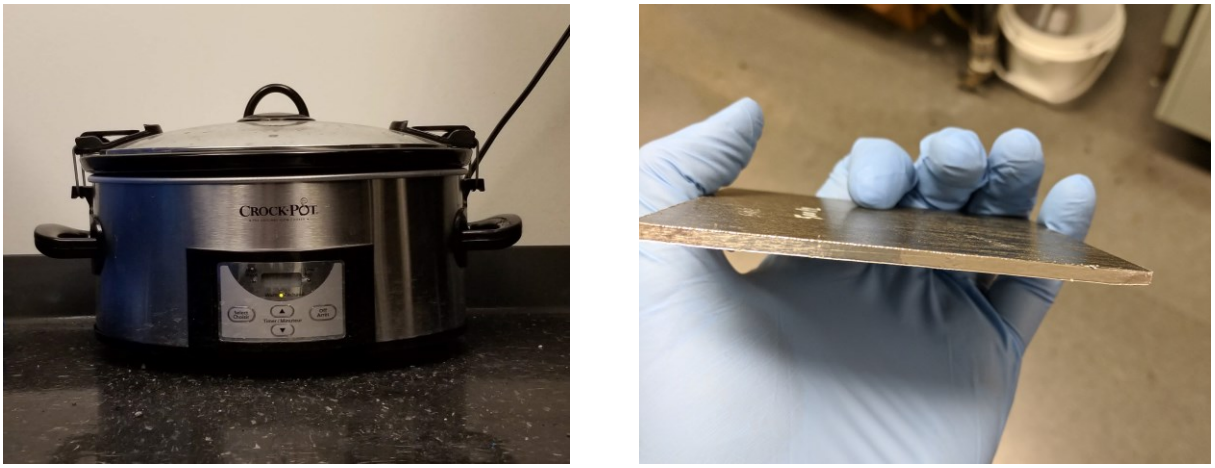

Figure 3-6 moisturising pot and the sample after adding aluminum foil to the edges

To find the correlation between moisture levels, void contents and the diffusivity of the composite samples, moisture absorption of carbon/epoxy samples were tracked based on ASTM D 5229/D 5229M standard and by immersing the samples in hot water at 60 ˚C [28, 57]. The amount of absorbed moisture was monitored by a scale with accuracy of 0.1 mg, using equation 6.

$$M, \% = \left(\frac{W_i - W_{Al}}{W_d}\right) * 100 \quad (6)$$

Where;

M is average moisture content

W_i is current sample mass [g]

W_d is oven dry sample mass [g]

W_{Al} is sample mass after adding steel foil [g]

Moisture absorption process stops when moisture level of composite laminate changes less than 0.01% at each time interval. At this level, the laminate reaches to state of moisture equilibrium. This can be described by equation 7.

$$\left|\frac{W_i - W_{i-1}}{W_d}\right| < 0.0001 \quad (7)$$

Where;

W_i is current sample mass [g]

W_{i-1} is sample mass at previous time interval [g]

And W_d is oven dry sample mass [g]

3.8 Material properties

3.8.1 Dynamic mechanical analysis

Dynamic mechanical analysis (DMA) is one of the most common experiments to measure the mechanical properties of wide ranging materials from low to high temperature. DMA can provide us valuable information such as storage modulus, loss modulus, damping factor and glass transition temperature.

Figure 3-7 shows the material response under sinusoidal loading for both pure solid and pure viscous materials. It can be seen, after applying the sinusoidal load, for the perfectly solid material the resulting strain would be in the same phase with the applied stress, while for the viscous material a 90-degree phase difference can be seen in the stress and resulting strain.

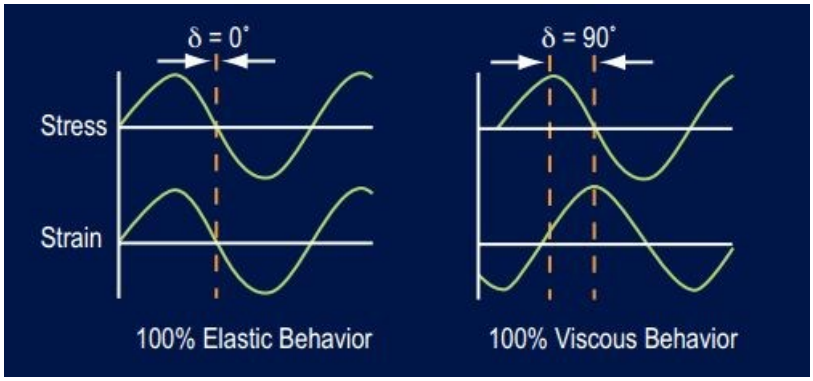

Figure 3-7 stress/strain response of pure elastic and pure viscous materials under sinusoidal loading [58].

On the other hand, a wide range of materials including polymeric composites are called viscoelastic materials which indicate both elastic and viscous behaviour with applying sinusoidal stress. Figure 3-8 indicates the viscoelastic behaviour of a viscoelastic material and mathematical relation between complex modulus (E^*), storage modulus (E'), loss modulus (E''), and damping factor (tan δ).

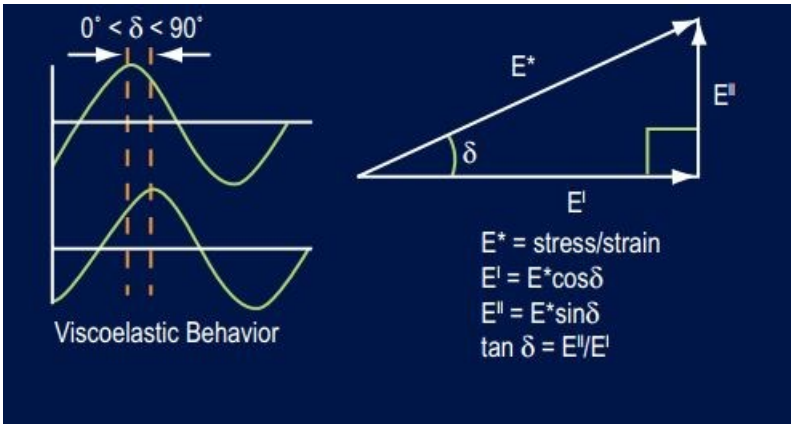

Figure 3-8 stress/strain relations of a viscoelastic material in sinusoidal loading [58].

Complex modulus is the stress over strain ratio and considering complex modulus and damping factor, we can find the storage modulus and loss modulus easily using above relations. The storage modulus is related to the stiffness of the composite laminate and exhibits the amount of

stored energy in the viscoelastic material which is related to the durability of the material under the loading. On the other hand, loss modulus represents the amount of energy which is dissipated through the molecules in the material. Damping factor is the ratio of loss modulus over the storage modulus which is a dimensionless number and shows the amount of lost energy in the composite material. DMA machine provides us with all these information as a function of temperature, frequency, and time [58, 59].

There are two main factors which make DMA test unique from other mechanical testing devices: first, usual tensile machines act only in elastic mode of the material while DMA observe both elastic and viscoelastic behaviour of the composite laminate. Second of all, typical tensile machine acts outside of the linear viscoelastic range while DMA machine measure the mechanical behaviour of laminate inside the linear viscoelastic region and that is why DMA is more sensitive to the structure of material.

In this study, DMA tests were performed using a TA instrument Q800 and at 3-point bending fixture which are shown in Figure 3-9. Dimensions of the samples were 50 mm × 10 mm × 3.5 mm and the fibers' directions were perpendicular to the length of the samples because considering the fact that moisture effects to the fibers are negligible, our interest was to study the change of matrix properties as the amount of absorbed moisture increase. In 3-point bending mode, the sinusoidal force is applied at the middle of the sample with frequency of 1 Hz while both ends of the samples are clamped. Using low friction roller bearings with high clamp span (almost 50mm) in the DMA tests, made the clamping effect negligible. The samples were heated from room temperature to 220 ˚C with increase ramp of 5 ˚/min.

Glass transition temperature is another valuable output from DMA tests. T_g is the temperature which the material goes from glassy state to the rubbery state with a sharp drop in stiffness. As temperature increases, the storage modulus of the sample decreases while loss modulus of the sample increases which can cause an increase in damping factor. T_g can be determined by the temperature at peak value of the tan δ curve [60].

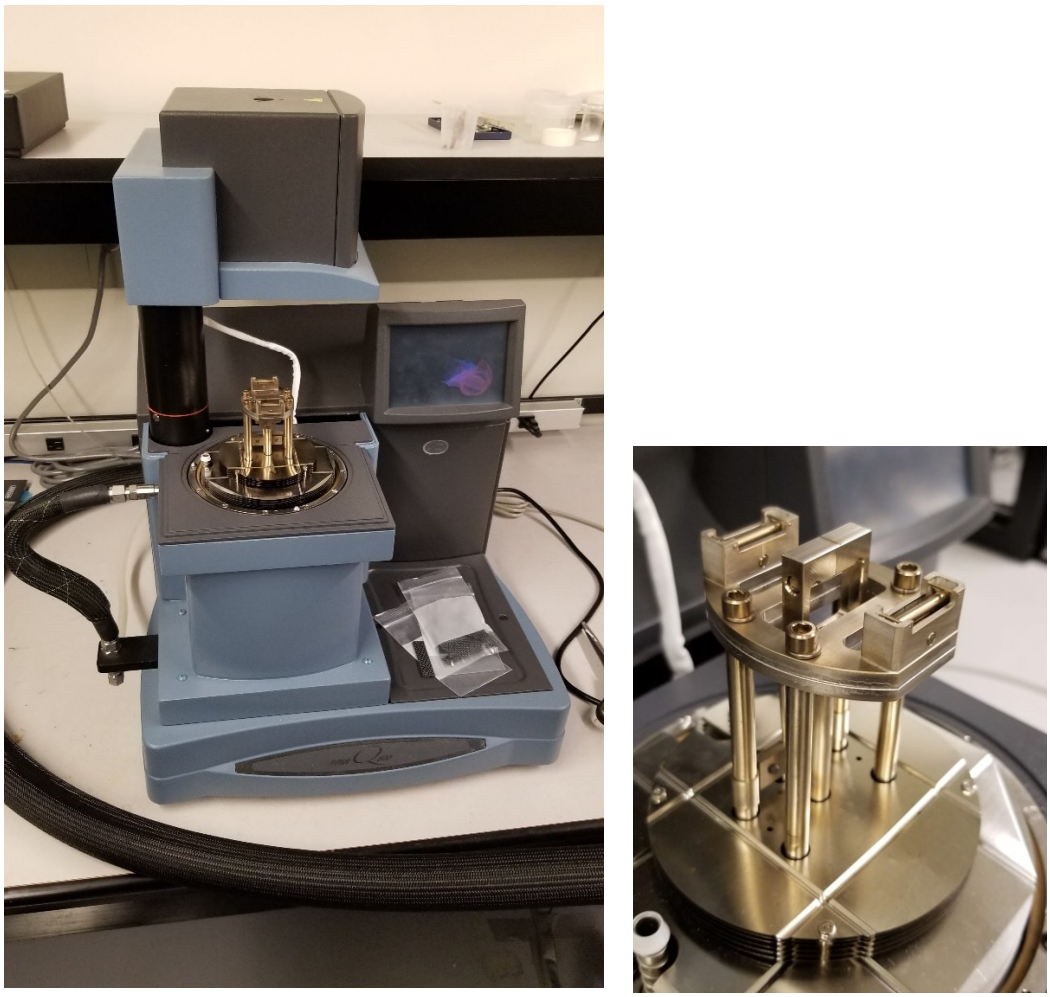

Figure 3-9 DMA machine and three point bending fixture

3.8.2 Interlaminar shear strength

The interlaminar shear strength test was described shortly in pervious chapter. In this study ASTM D2344 standard test method was followed to conduct the ILSS tests at three point bending mode at room temperature and 50% relative humidity. Z5 single column tensile tester was used with the Wyoming three point bending fixture to perform the ILSS tests. Figure 3-10 shows the ILSS test machine installing the three point bending fixture. According to the ASTM standard and based on the specimen's dimensions, span length of the machine was 14mm and the tests were run with the crosshead speed of 1 mm/min.

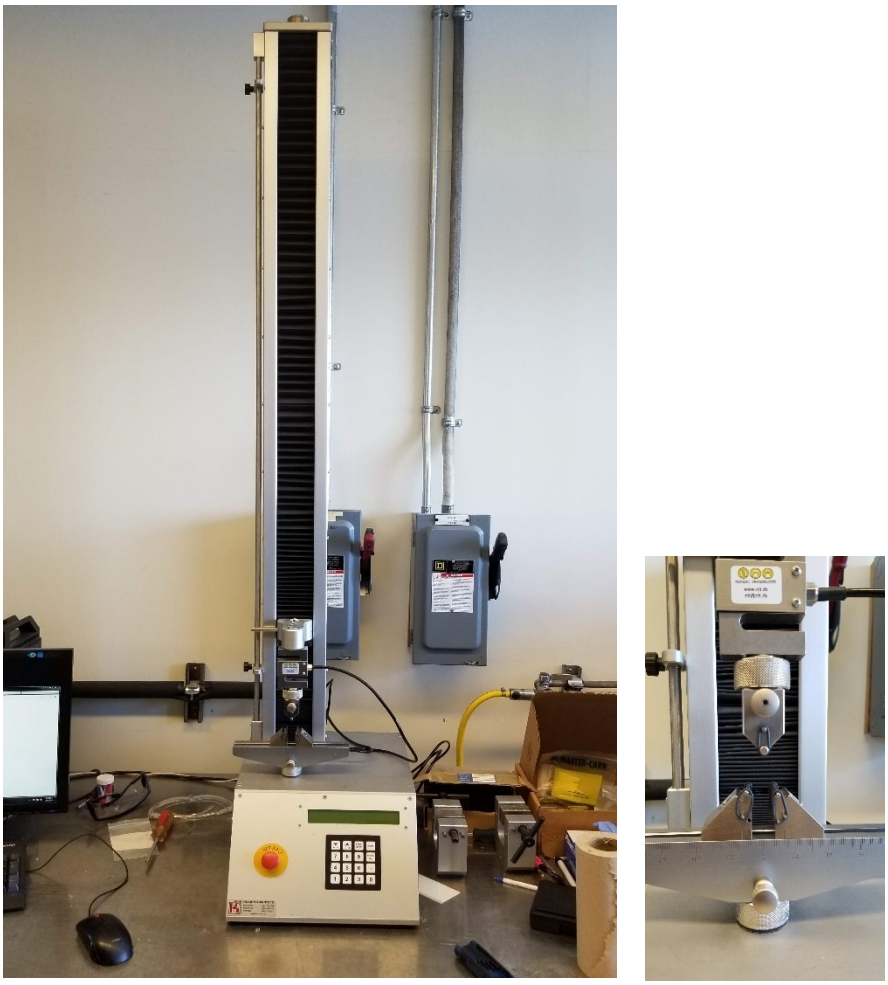

Figure 3-10 Z5 single column tensile tester machine and Wyoming three point bending fixture

Chapter 4

4 Results and discussion

4.1 Moisture absorption-Diffusivity

The procedure proposed by ASTM was followed to run the moisture tests and to analyze the data [28]. The sample weights of six unidirectional carbon/epoxy laminates at three different void contents were measured and recorded during different intervals within one year exposure time (the provided results are average of two specimens). The Moisture content was calculated from change of weight. The results are shown in Figure 4-1. As it can be seen, the moisture absorption for all laminates was linear up to almost 1.6% moisture level. After that, there is a change in slope of the moisture absorption which illustrates the laminates are getting saturated. For the laminate with the lowest void content, the weight change is less, compare to the laminate with the highest void content. This might be related to the void effect. Up to 1.6% moisture absorption, the resin might get saturated and then the water might start to fill the void areas more.

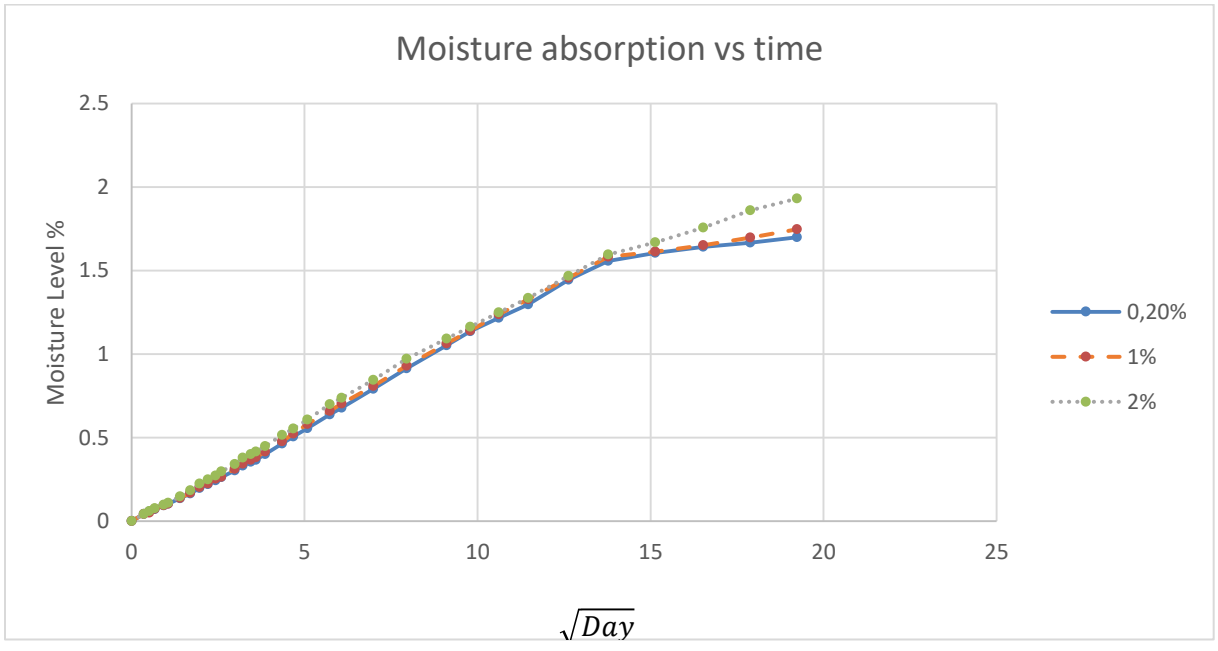

Figure 4-1 experimental data from moisture absorption process of composite laminates at three different levels of void content

In this research in order to calculate the diffusivity, the last weighted sample after one year represents the maximum level of absorbed moisture due to the time limitation. According to the experimental data, increasing the void volume fraction of laminates led to an increase in the amount of absorbed moisture. Using Fick's law and ASTM standard method, equation 4 should be used to determine the diffusivity.

The second parenthesis in equation 4 represents the slop of the experimental results at the linear section of the data. Figure 4-2 shows the variation of the moisture contents with time for three different void levels at linear section. The slop of the data was calculated using the best linear fit to the data. The slop, thickness, and effective moisture equilibrium content M_m, and diffusivity for each case are shown in Table 4-1.

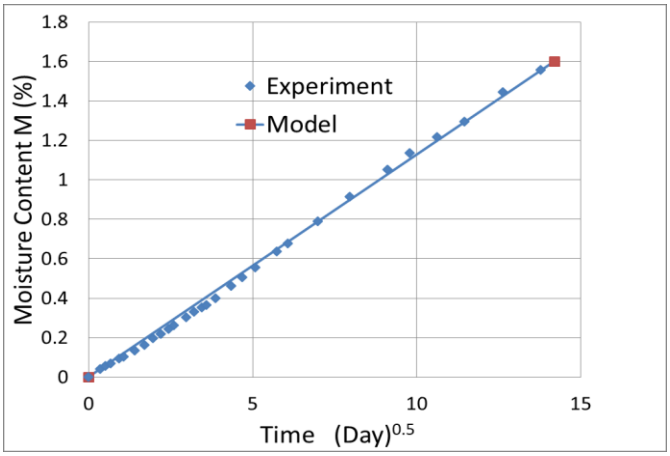

(a)

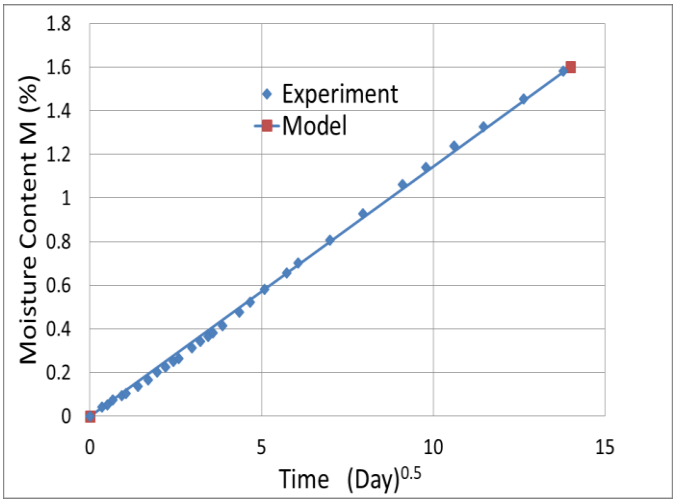

(b)

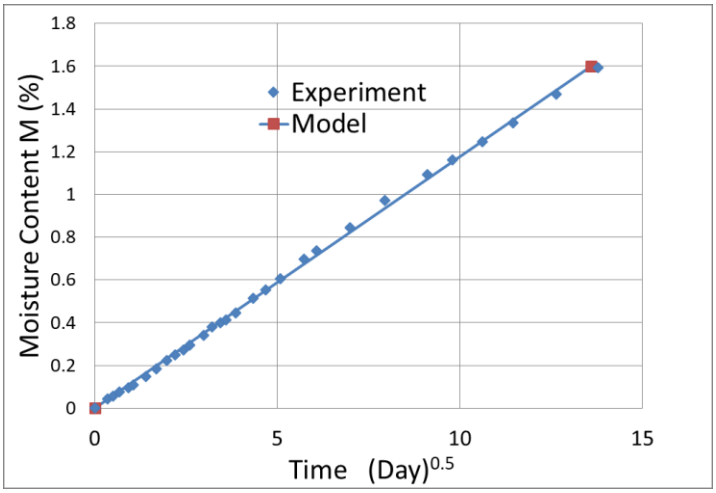

(c)

Figure 4-2 Moisture content vs time for three different void contents a) 0.2% b) 1% c) 2%

Table 4-1 Diffusivity for samples containing three different void levels

Void Volume Fraction (%)	Sample Thickness (*mm*)	M_m *(%)*	Slope $\left(\frac{M_2 - M_1}{\sqrt{t_2} - \sqrt{t_1}}\right)$	Diffusivity D_x *(mm²/sec)*
0.2	3.4	1.699	$3.8\text{x}10^{-4}$	$1.161\text{x}10^{-7}$
1	3.5	1.746	$3.9\text{x}10^{-4}$	$1.202\text{x}10^{-7}$
2	3.9	1.930	$4.0\text{x}10^{-4}$	$1.243\text{x}10^{-7}$

As can be seen, the diffusivity increases by level of voids and in fact will be a function of void level (Figure 4-3). In order to find a mathematical expression and function to describe the variation of diffusivity vs void contents more data is required. However, it can be concluded that within the range of experiment, the behaviour can be assumed to follow a quadratic function as:

$$D_x = av^2 + bv + c \tag{8}$$

Where v stands for void volume fraction.

Using curve fitting, the diffusion coefficient can be calculated at each void level using following parameters:

$a = -6E - 10$

$b = 6E - 9$

, and $c = 1E - 7$.

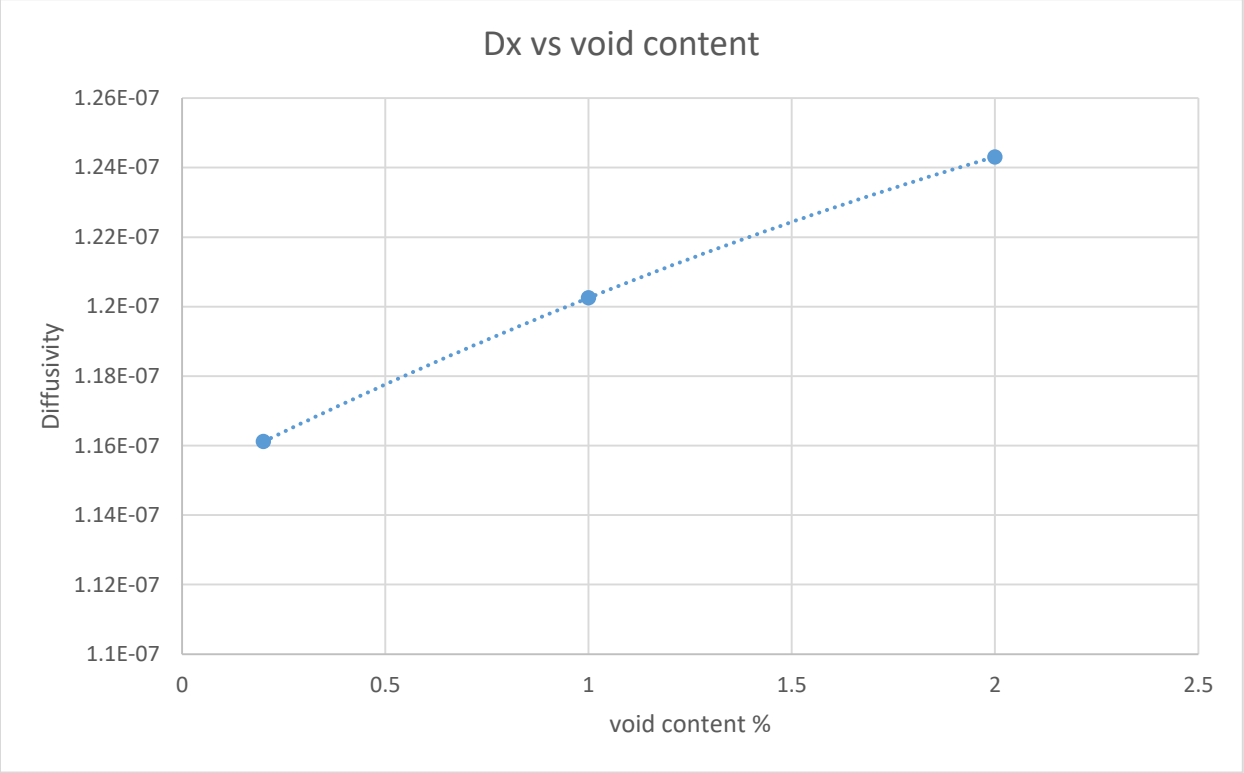

Figure 4-3 diffusivity and void content relations based on experimental data

4.2 Interlaminar shear strength

4.2.1 Samples with 0.2% void content

To study the shear strength of matrix layers, interlaminar shear strength (ILSS) test was done on unidirectional laminate composites at different levels of moisture and void contents. At this step, Figure 4-4 displays a typical force-displacement plot for the samples with minimum void content at dry level before moisturising. Maximum bearable load reported for this sample was 3058 N. Different acceptable modes of failure according to ASTM D2344 and actual failure modes are shown in *Figure 4-5*.

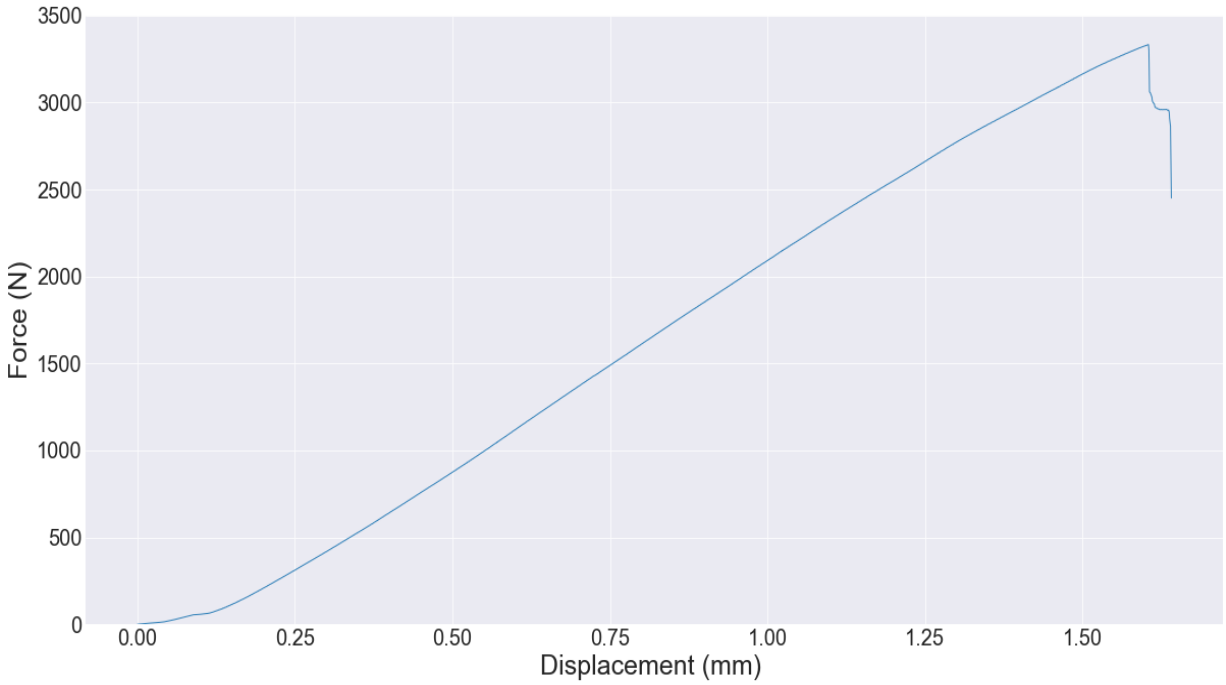

Figure 4-4 force-displacement plot for ILSS test of a unidirectional composite laminate with minimum void content before exposing to moisture environment.

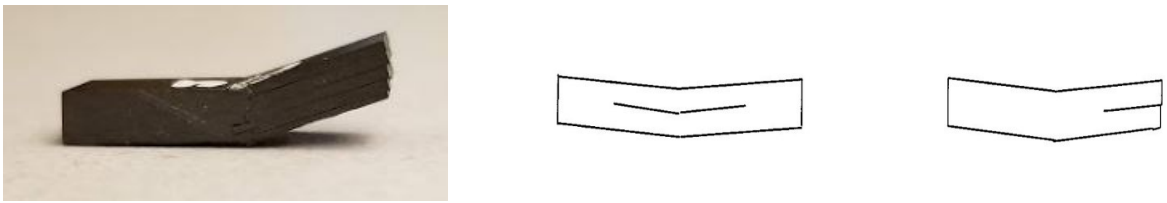

Figure 4-5. A unidirectional laminate after short beam test (the left picture), and two acceptable modes of failure for Interlaminar shear test based on ASTM D2344 (two pictures on the right)

Figure 4-6 shows how ILSS varies for the composite laminate after exposure of samples to the moisture environment. Results are the average of three (3) specimens. The ILSS for the samples first increased gradually from 103 MPa to 103.6 MPa after absorbing 0.4% moisture. Then, it dropped sharply, about 12.5%, to 90.6 MPa, after absorbing 0.8% moisture. After absorbing 1.2% moisture, the ILSS faced almost 3% drop at the end. To have a better understanding, Table 4-2 indicates the change rate of ILSS as moisture absorption increased.

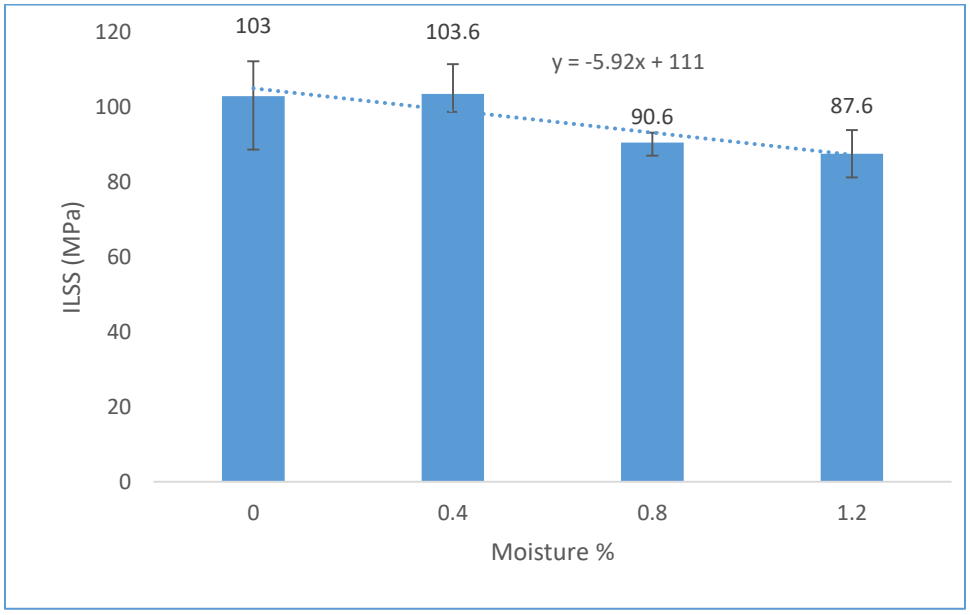

Figure 4-6 Interlaminar shear strength of unidirectional laminates containing 0.2% void content subjected to four different moisture level

Table 4-2 summary of ILSS and change rate of unidirectional laminates containing 0.2% void content subjected to four different moisture level

Moisture Level	ILSS(MPa)	CR compare to previous step	CR compare to dry condition
0	103	n/a	0
0.4	103.6	0.58	0.58
0.8	90.6	-12.54	-12.03
1.2	87.6	-3.31	-14.95

4.2.2 Samples with 1% void content

Figure 4-7 indicates a typical force-displacement plot from a short beam test of carbon/epoxy laminates with 1% void content before moisturising procedure at dry condition. The maximum tolerable load before breakage for this sample was 2998.25 N and the load decreased instantaneously because of interlaminar shear failure.

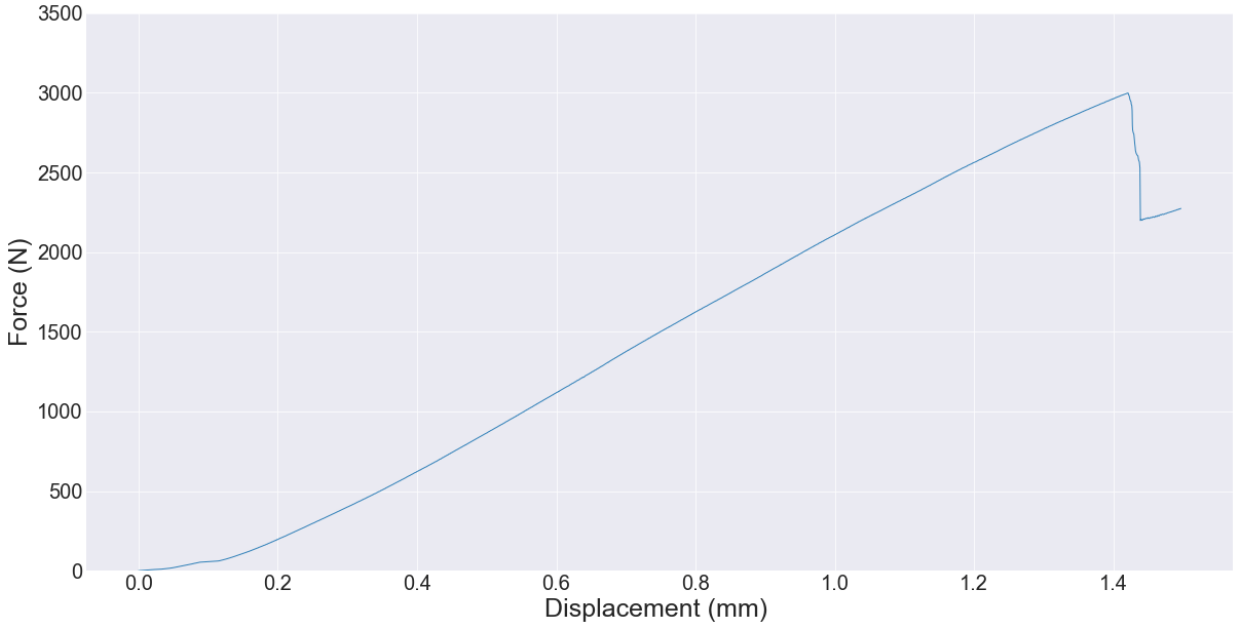

Figure 4-7 force-displacement plot for ILSS test of a unidirectional composite laminate with 1% void content before exposing to moisture environment

From the graph below, it is evident that from dry condition to 1.2% moisture level, there is a variation of ILSS for samples containing 1% void content. Surprisingly, ILSS was found to increase by 8.7% from 95 MPa to 103.3 MPa after absorbing 0.4% moisture. Next, after absorbing 1.2% moisture, ILSS reduced by 17.39% from 103.3 MPa to 85.33 MPa. To summarize, the change rates of ILSS for composite laminates with 1% void content are listed in *Table 4-3*.

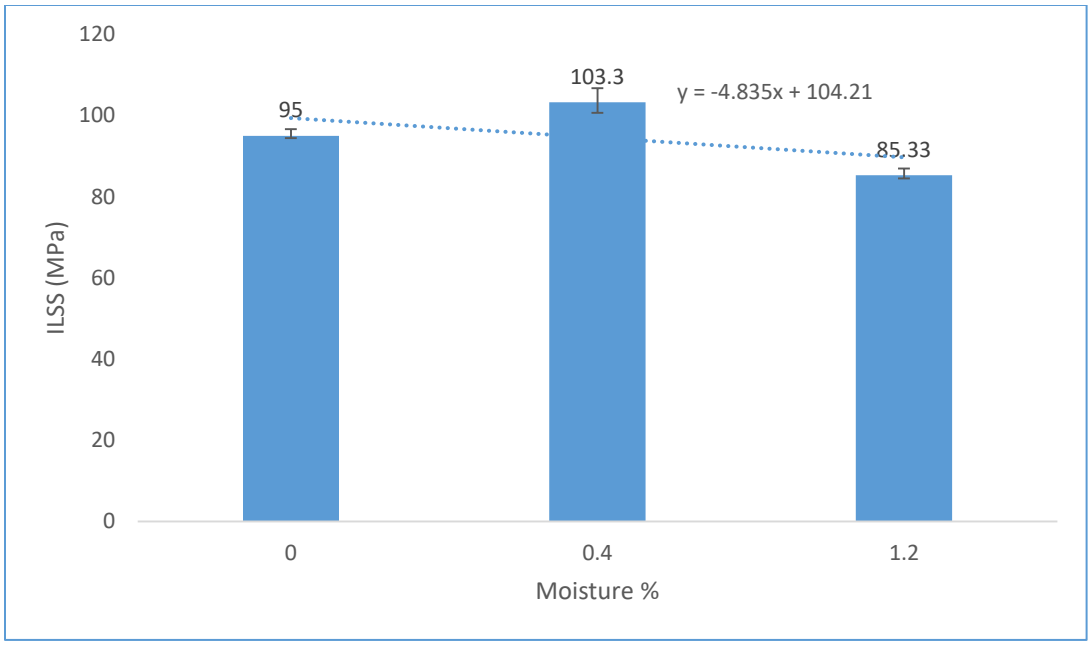

Figure 4-8 Interlaminar shear strength of unidirectional laminates containing 1% void content subjected to four different moisture level

Table 4-3 summary of ILSS and change rate of unidirectional laminates containing 1% void content subjected to four different moisture level

Moisture Level	ILSS(MPa)	CR compare to previous step	CR compare to dry condition
0	95	n/a	0
0.4	103.3	8.74	8.74
1.2	85.33	-17.39	-10.18

4.2.3 Samples with 2% void content

Figure 4-9 demonstrates a common force-displacement curve gained from three point bending test of current carbon/epoxy laminate, holding 2% void content at dry condition. The maximum bearable load for specimen was 2608 N followed by a sharp drop caused by ILSS failure.

Figure 4-10 presents change of the ILSS of the composite laminates at this level of void content versus absorbed moisture. Comparing the ILSS at dry condition and after absorption of 0.4% moisture, ILSS dropped gradually about 2% from 87.60 MPa to 85.83 MPa. Next, with the absorption of an additional 0.4% moisture, ILSS dropped by almost 8% from 85.83 MPa to 79

MPa. At the end, when samples absorbed 1.2% moisture, a further 2.5% drop, from 79 MPa to 77 MPa, was observed. *Table 4-4* shows a brief summary of ILSS and its change rate versus moisture levels.

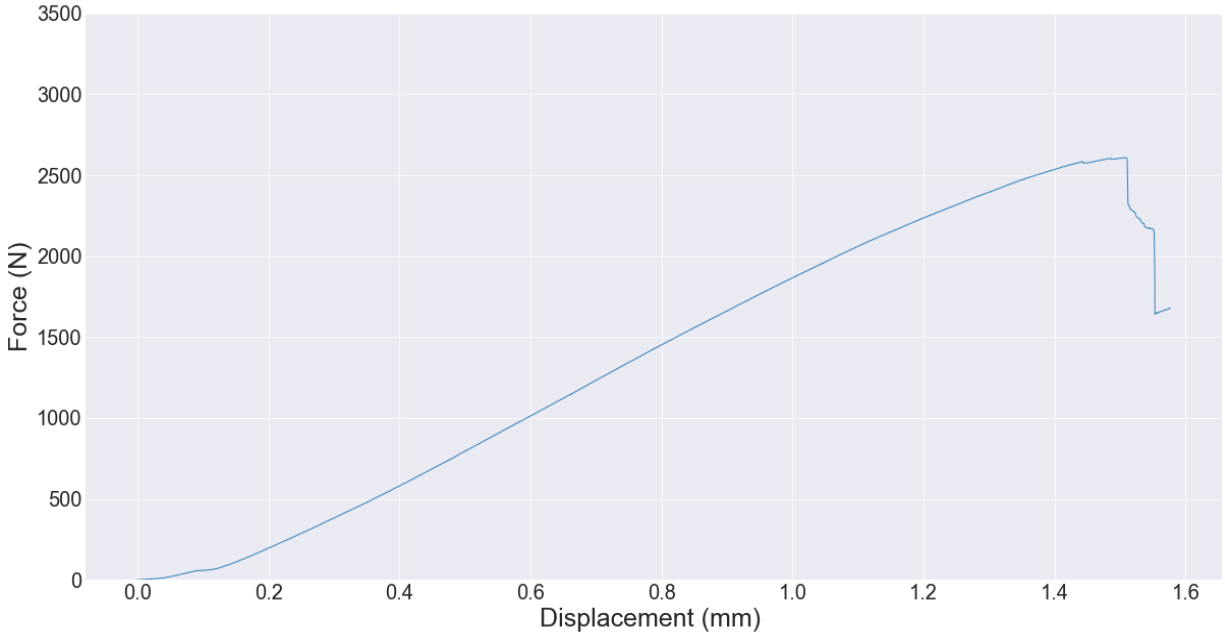

Figure 4-9 force-displacement plot for ILSS test of a unidirectional composite laminate with 2% void content before exposing to moisture environment

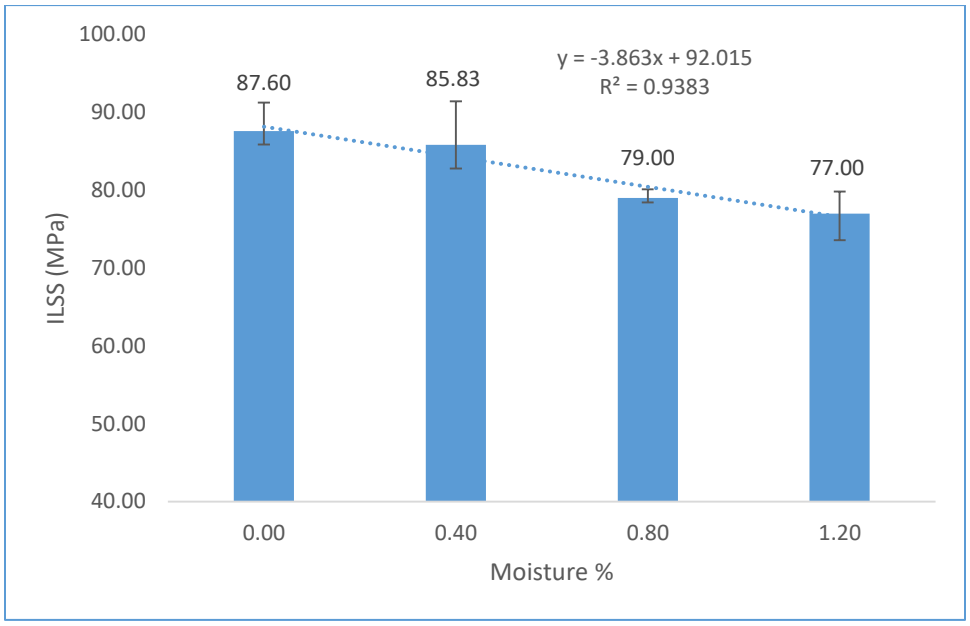

Figure 4-10 Interlaminar shear strength of unidirectional laminates containing 2% void content subjected to four different moisture level

Table 4-4 summary of ILSS and change rate of unidirectional laminates containing 2% void content subjected to four different moisture level

Moisture Level	ILSS(MPa)	CR compare to previous step	CR compare to dry condition
0.00	87.60	n/a	0.00
0.40	85.83	-2.02	-2.02
0.80	79.00	-7.96	-9.82
1.20	77.00	-2.53	-12.10

4.3 Discussion

There are some factors which can affect our experimental results and it is important to find the connection between these affecting factors. Moisture absorption can change the mechanical properties of CFRPs in different ways:

- Extra crosslinking: to do the moisturising, samples were kept in the hot water at 60 ˚C. Samples at higher moisture levels were immersed in water for longer period which can lead to extra cross-linking in polymer chains.
- Non uniform voids: although microscopic observations showed uniform void distribution between the prepreg layers, there may be non-uniform void contents at inner surfaces or also other sections which are not monitored by microscope.
- Change in molecular chains: water molecules increase the plasticization property of the material by penetrating through the polymer chains which can have softening effects and lead to a reduction in mechanical properties.

As another method of assessment, the joint effect of moisture and void content on ILSS is presented. First, the “Curve Fitting Toolbox” of Matlab software was used to find a two-variable function to represent the relationship between all variables. In this section, the input-output relationship was assumed to be polynomial. Different orders for the dependent variables, i.e. moisture level m and void content v, were tested while assuming ILSS as the dependent output variable.

Different sets of experiments proved that the second-order polynomial was the best model. In the following, the estimated polynomial representation is presented:

$$ILSS = a_0 + a_1 v + a_2 m + a_3 v^2 + a_4 vm + a_5 m^2 \quad (9)$$

Where the polynomial parameters are estimated as the following:

a_0 =109.3, a_1 =-19.96, a_2 =-15.38, a_3 = 2.708, a_4 =3.003, and a_5 =2.675.

To visualize this joint effect, Figure 4-11 was plotted, which is a visual illustration of equation 8. This figure visualizes ILSS with a heat map in which yellow outputs represent higher ILSS and blue outputs represent low ILSS. As can be seen, the increase of moisture level and void content decrease ILSS drastically, which is an empirical demonstration of the hypothesis.

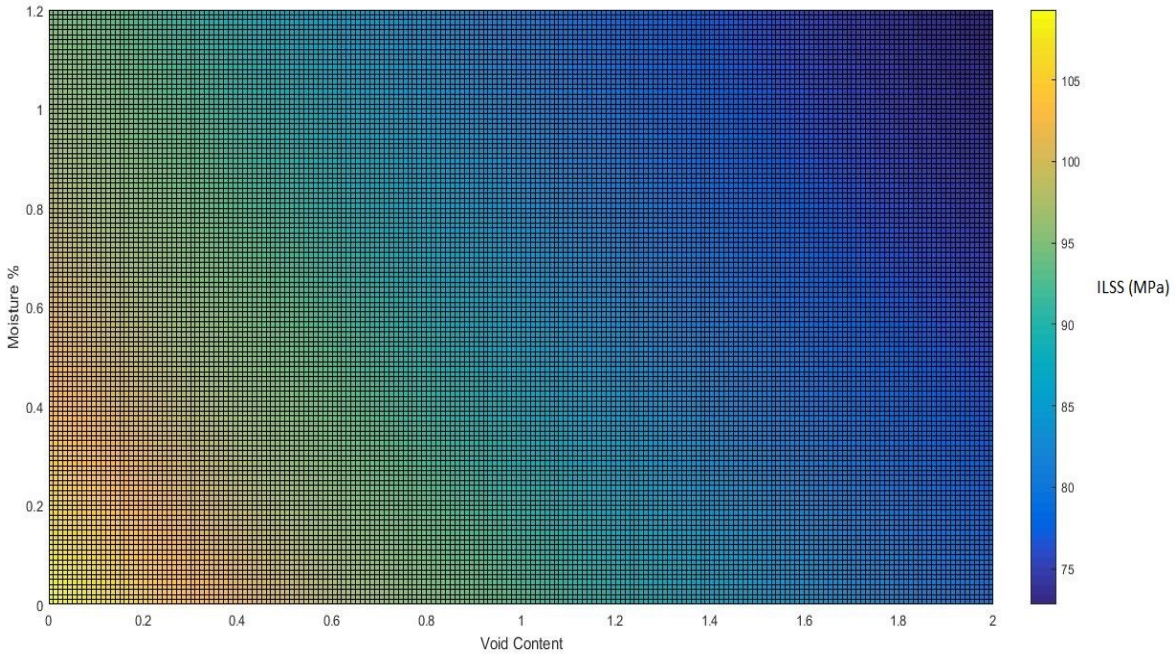

Figure 4-11 visual explanation of effect of void content and absorbed moisture on interlaminar shear strength of unidirectional laminate.

4.4 Moisture effects on Dynamic Mechanical properties

Dynamic Mechanical Analysis (DMA) was performed to measure change of storage modulus (E′), loss modulus (E″), tan δ, and glass transition temperature (T_g) of the samples at dry level and after being exposed to moisture. The viscoelastic behaviour of the polymer is studied by conducting DMA tests while the storage modulus represents the elastic section by measuring

stored energy and the loss modulus represent viscous portion by studying the amount of energy dissipated as heat in the sample[61]. The following results are the average of two different specimens.

4.4.1 Samples with 0.2% void content

Figure 4-12 indicates dynamic mechanical properties of unidirectional samples at dry condition. Variation of storage modulus, loss modulus, and tan δ from room temperature to 250 ˚C are visible in the graph. As it is shown in the graph, storage modulus (E′) of the UD laminate decreased slightly as temperature increased, which indicates the laminate became less elastic. From 25 ˚C to 160 ˚C storage modulus decreased by almost 12.5%. A dramatic decline in E′ can be seen from 160 ˚C to 250 ˚C which is a proof that the samples are in a rubbery state.

With increasing the temperature, the value of loss modulus and tan δ increased gradually and they decreased after a sharp increase.

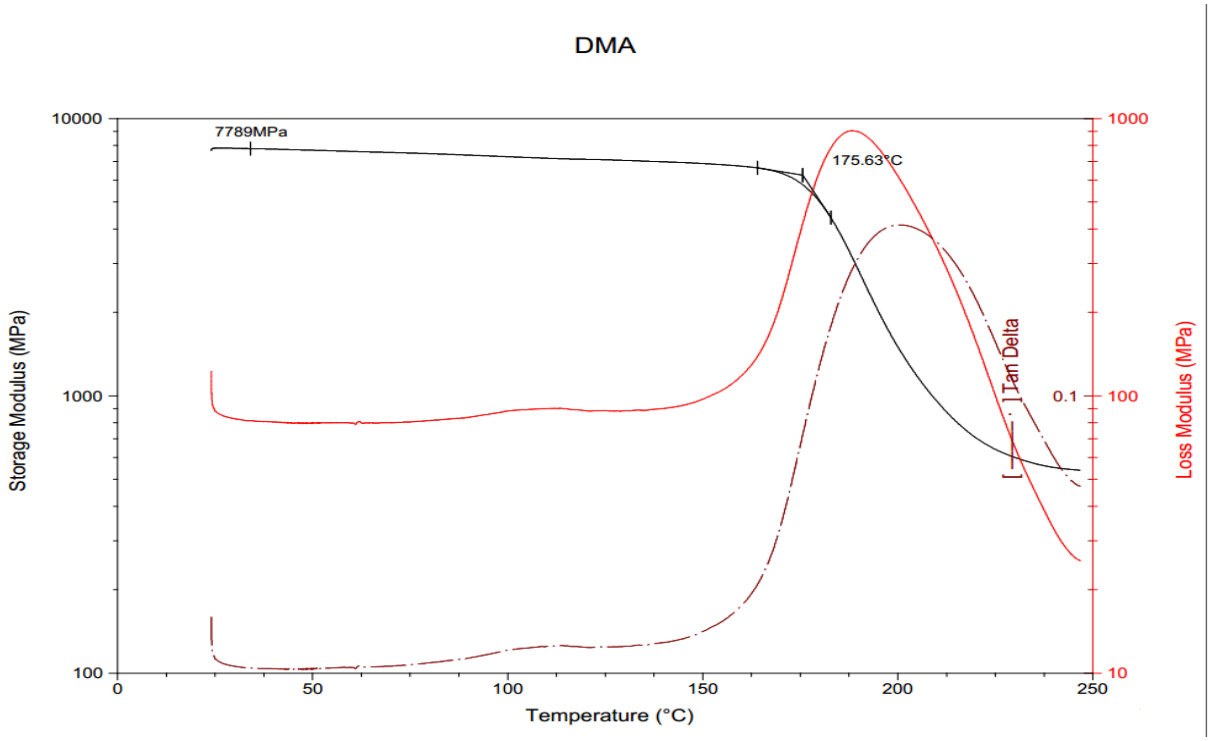

Figure 4-12 Dynamic mechanical analysis of UD samples at minimum level of void content vs temperature at Dry condition

4.4.1.1 Effect of moisture on storage modulus

The effects of penetrated moisture on the storage modulus of unidirectional carbon/epoxy laminates are shown in Figure 4-13. There is a clear trend of reduction in storage modulus as the amount of absorbed moisture increased despite one fluctuation at the end. From this data, it is clear that moisture affected glass transition temperature significantly and laminates reached the Tg at lower temperature, as the amount of absorbed moisture increased. To make it easier, Figure 4-14 shows the storage modulus of laminates at 25 ˚C for all levels of moisture.

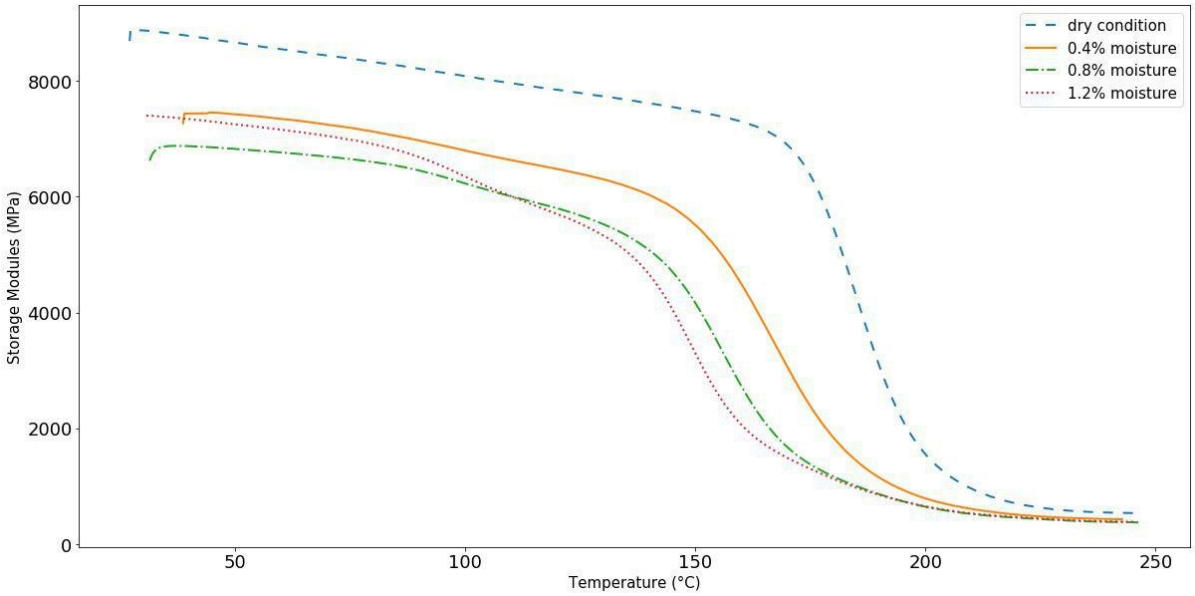

Figure 4-13 moisture effect on storage modulus of UD samples with 0.2% void content vs temperature at 90 ˚ direction

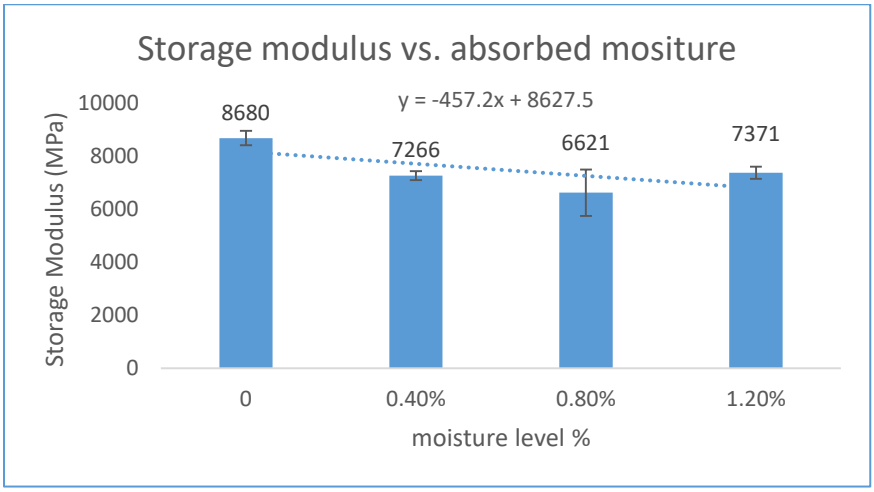

Figure 4-14 change of storage modulus of UD samples with 0.2% void content at 90 ˚ at room temperature for different levels of moisture

4.4.1.2 Effect of moisture on loss modulus

Using DMA test, the loss modulus of laminates after exposure to moisture can be accessed, as shown in Figure 4-15. Loss modulus illustrates the mechanical energy which is dissipated through the sample and the maximum value is related to the molecular friction after reaching the T_g.

Peak values in all different moisture levels are presented. As Figure 4-15 shows, there is a significant drop (almost 35%) in peak value after absorbing 0.4 % moisture while with increasing moisture level from 0.4% to 1.2%, the peak value remained almost constant. Interestingly, there is a left shift in peak values on the temperature axis, which again refers to reduction in T_g after absorbing moisture.

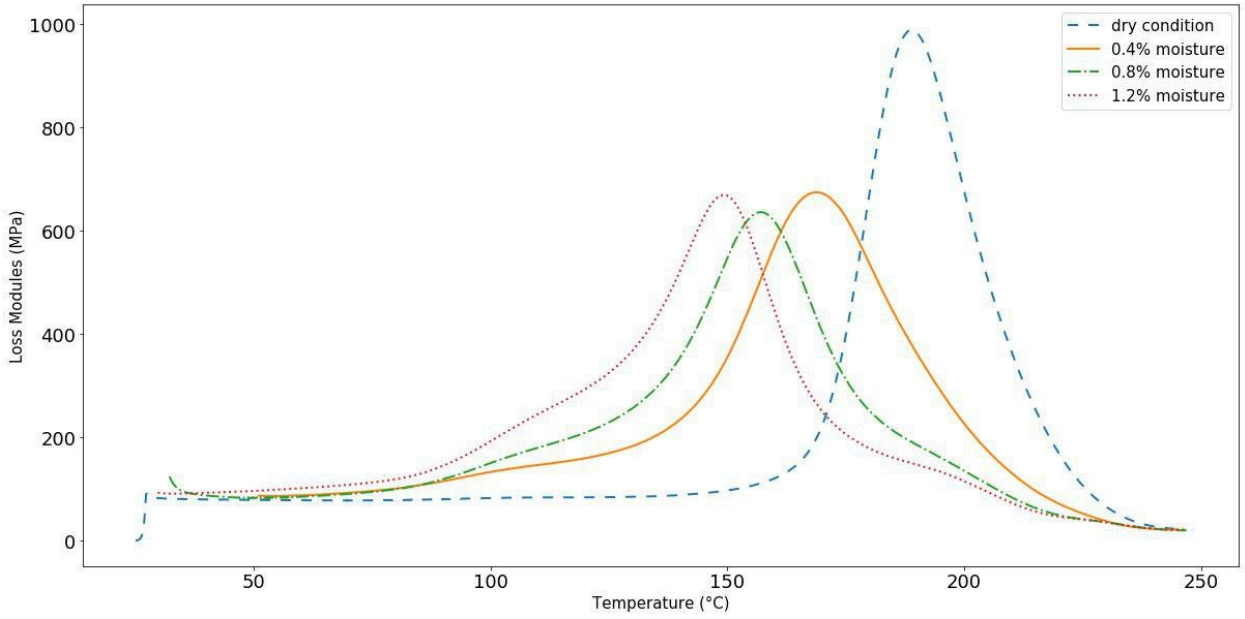

Figure 4-15 variation of loss modulus of UD samples with 0.2% void content for all levels of moisture in 90˚ direction

4.4.1.3 Effect of Moisture on Tan δ

Tan δ refers to the ratio of loss modulus to storage modulus. *Figure 4-16* indicates the variation of tan δ for the unidirectional laminates at dry condition and three different levels of moisture. After absorbing 0.4% moisture, tan δ dropped by almost 25%. Tan δ continuously reduced as temperature increased and reached a minimum at 1.2% moisture level.

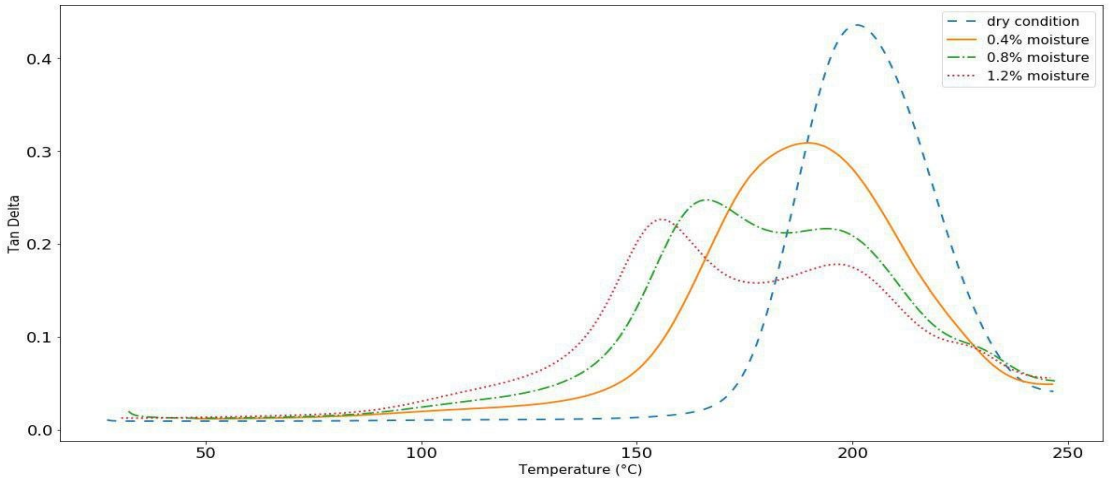

Figure 4-16 variation of Tan δ for UD samples with 0.2% void content at 90˚ direction with increase in amount of absorbed moisture

4.4.1.4 Effect of moisture on glass transition temperature

Glass transition temperature (T_g) is another remarkable output of DMA tests. Although T_g can be presented using storage modulus, loss modulus, and tan δ plots versus temperature, it is preferred to use tan δ graphs in the literature. To have a better look and understanding, variation of T_g for all moisture levels are provided in *Figure 4-17*. It is clear that T_g tends to reduce continuously with increasing moisture level because water acts as a potent plasticizer [62]. It can be seen that after absorbing 1.2% moisture, T_g dropped by almost 23%. The same trend is reported by other researchers as well [63].

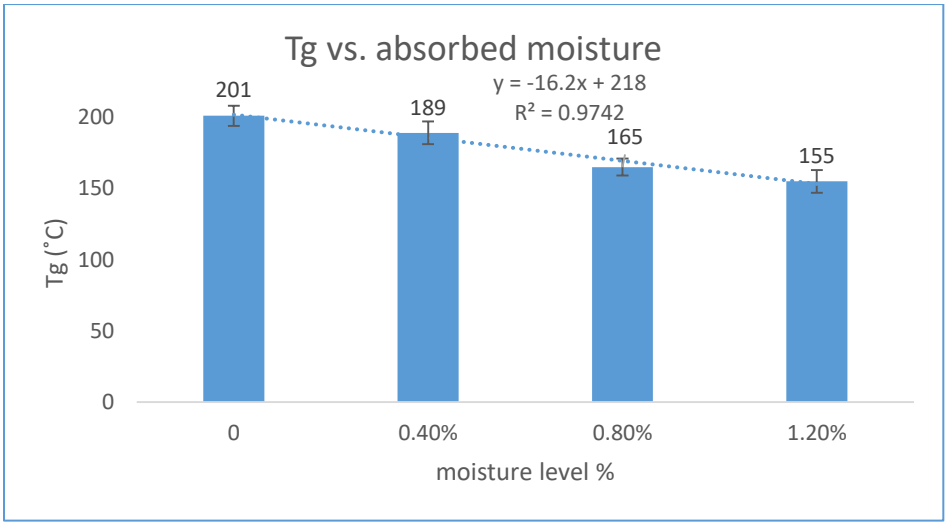

Figure 4-17 change of glass transition temperature with increase in amount of absorbed moisture for UD samples with 0.2% void content

4.4.1.5 DeBenedetto equation

During the manufacturing of thermosetting composite materials, as the degree of cure and crosslinking increases, the glass transition temperature increases. For many thermosetting systems, the relationship between glass transition temperature Tg and degree of cure (α) can be described by the empirical DiBenedetto equation as [64]:

$$\frac{T_g(\alpha) - T_g(0)}{T_g(\infty) - T_g(0)} = \frac{\lambda\alpha}{1-(1-\lambda)\alpha} \tag{10}$$

Where $T_g(0)$ is the glass transition temperature of the uncured resin, $T_g(\infty)$ is the glass transition temperature of the fully cured material, and λ is a material constant. This equation is fitted to the experimental data to obtain $T_g(\infty)$, $T_g(0)$ and λ.

When the thermosets absorb the moisture, the presence of water molecule inside the resin molecular structure has softening effect and therefore the glass transition temperature drops. This behavior is opposite to the curing process. However, through analogy, the form of the DiBenedetto equation can be adopted to capture the variation of the glass transition temperature vs moisture content (M). The modified DeBenedetto equation can be expressed as

$$\frac{T_g(M) - T_g(D)}{T_g(\infty) - T_g(D)} = \frac{\lambda M}{1-(1-\lambda)M} \tag{11}$$

Where $T_g(D)$ is the glass transition temperature of the completely dried resin, $T_g(\infty)$ is the glass-transition temperature of the fully saturated resin, and λ is a material constant. M is the moisture content (%). This equation was fitted to the experimental data to obtain $T_g(D)$, $T_g(\infty)$ and λ. The results are shown in the following and Figure 4-18:

$$T_g(D) = 207\ ^\circ C$$
$$T_{g\infty} = 150\ ^\circ C$$
$$\lambda = 1.45$$

By having the level of moisture, the glass transition temperature can be predicted.

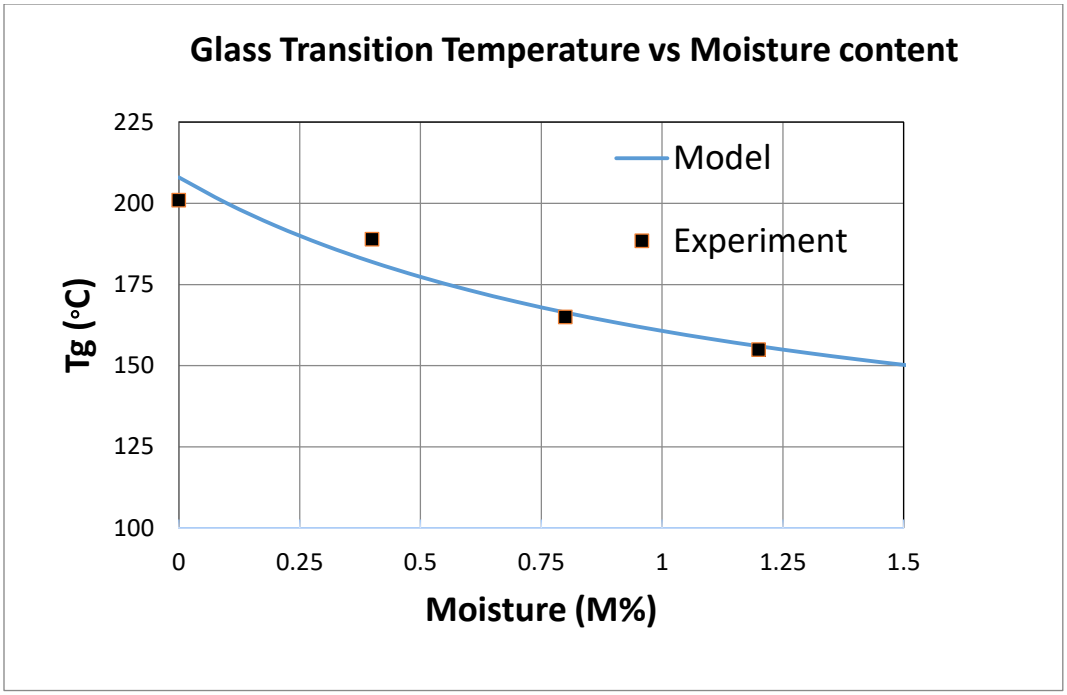

Figure 4-18 Variation of glass transition temperature vs level of moisture using proposed modified Dibenedetto equation

4.4.2 Samples with 1% void content

To study the variation of storage modulus, loss modulus, tan δ, and T_g of the unidirectional laminate containing 1% void content, dynamic mechanical analysis was conducted. The following results are an average of two different specimens.

DMA results of UD carbon/epoxy laminates with 1% void content before moisturising are displayed in Figure 4-19. The variation of storage modulus, loss modulus, and tan δ versus temperature in the range of 25 ˚C to 250 ˚C are provided. Like previous samples with lower void content, storage modulus reduced as temperature increased. At 178 ˚C, storage modulus dropped sharply because the laminate was transitioning into a rubbery state. Also loss modulus and tan δ first increased with increasing temperature and reached a peak value. Then both reduced drastically as temperature increased.

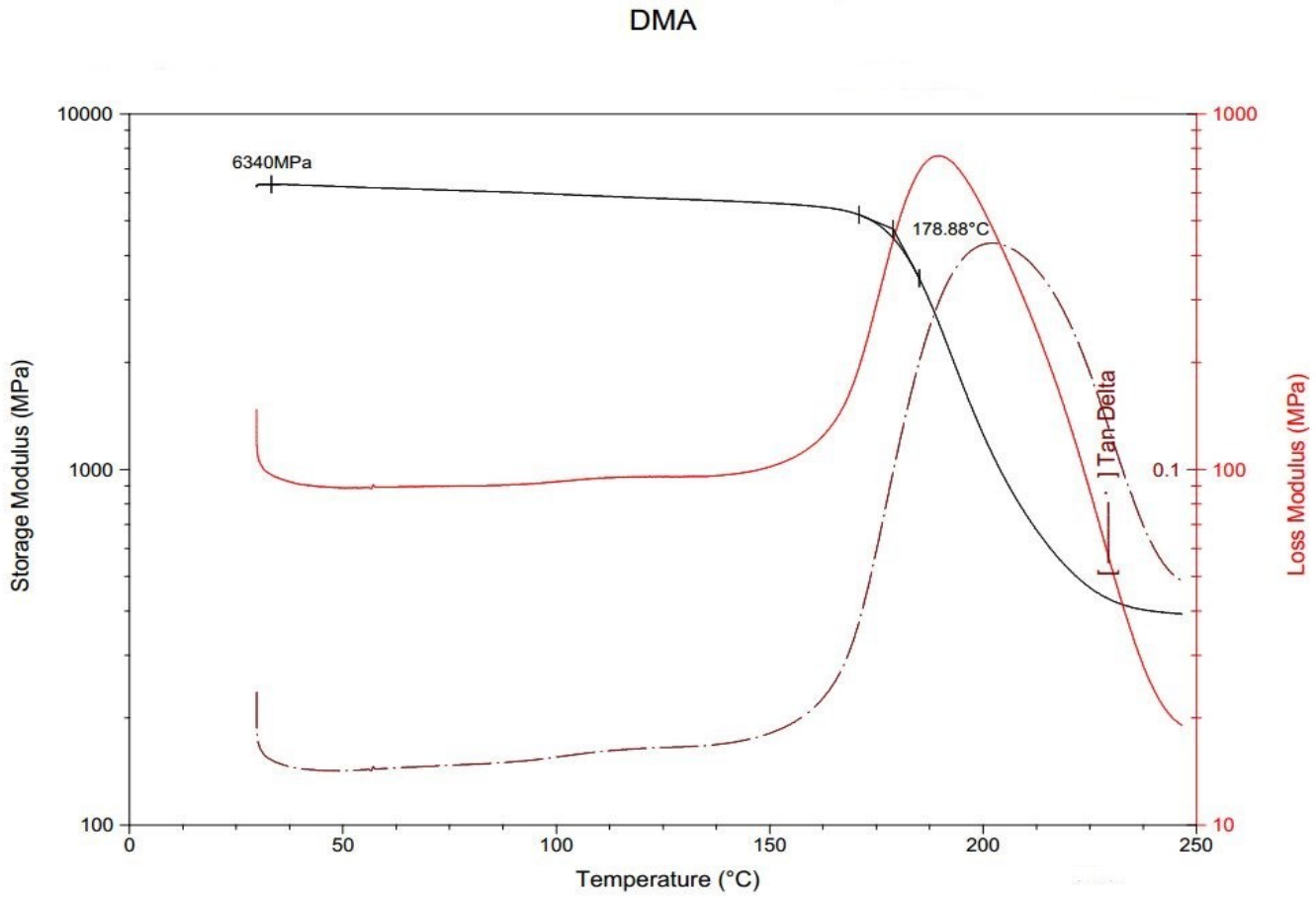

Figure 4-19 Dynamic mechanical analysis of UD samples with 1% void content vs temperature at Dry condition

4.4.2.1 Effect of moisture on storage modulus

Figure 4-20 shows the variation of storage modulus of UD laminates containing 1% void content against temperature for three different moisture levels. Storage modulus reduced as the amount of absorbed moisture increased in composite laminates. It can be seen that storage modulus reduced by almost 10% after absorbing 1.2% moisture.

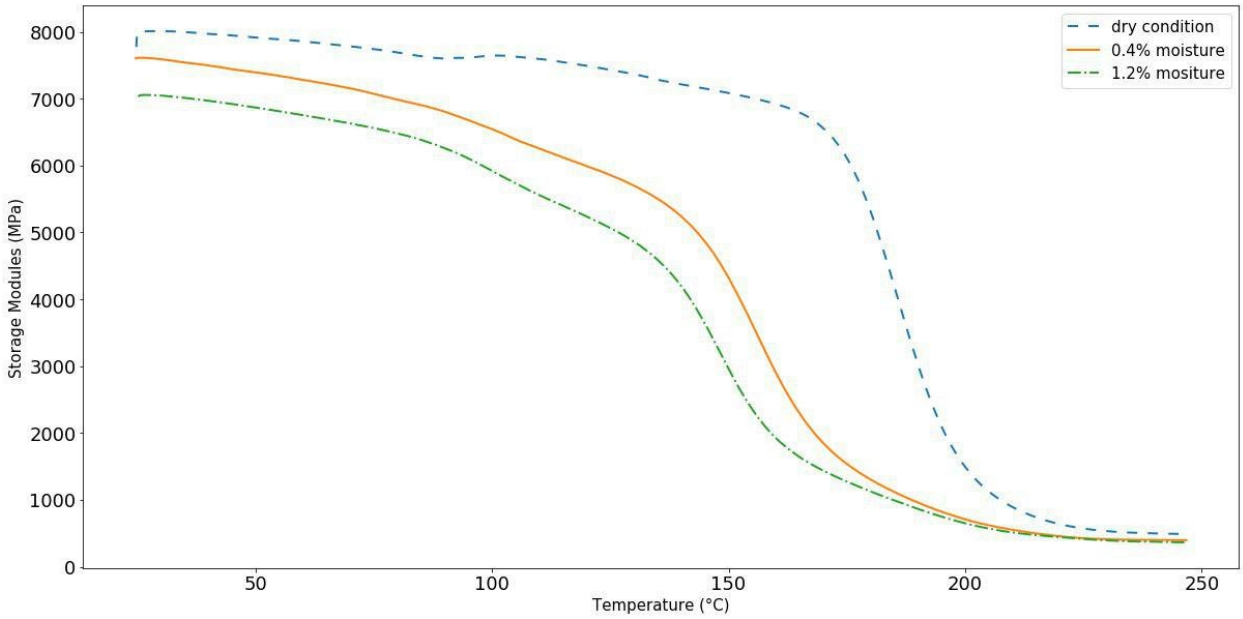

Figure 4-20 moisture effect on storage modulus of UD samples with 1% void content vs temperature at 90 ˚ direction

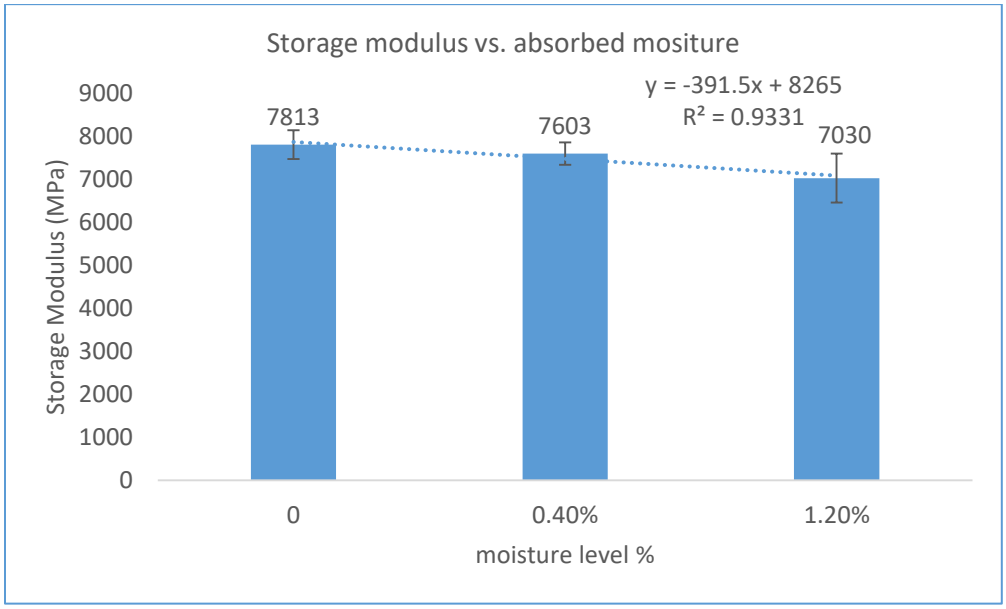

Figure 4-21 change of storage modulus of UD samples with 1% void content at 90 ˚ at room temperature for different levels of moisture

4.4.2.2 Effect of moisture on loss modulus

Figure 4-22 indicates moisture absorption effect on loss modulus of carbon/epoxy samples having 1% void content. Checking the peak points of the graph, a sharp drop in loss modulus by about 20%, from 850 MPa to 670 MPa, can be seen after the absorption of 0.4% moisture.

However, after this level, the reduction rate of the loss modulus became slower and finally E″ dropped to 590 MPa, which shows 30% reduction compared to dry condition.

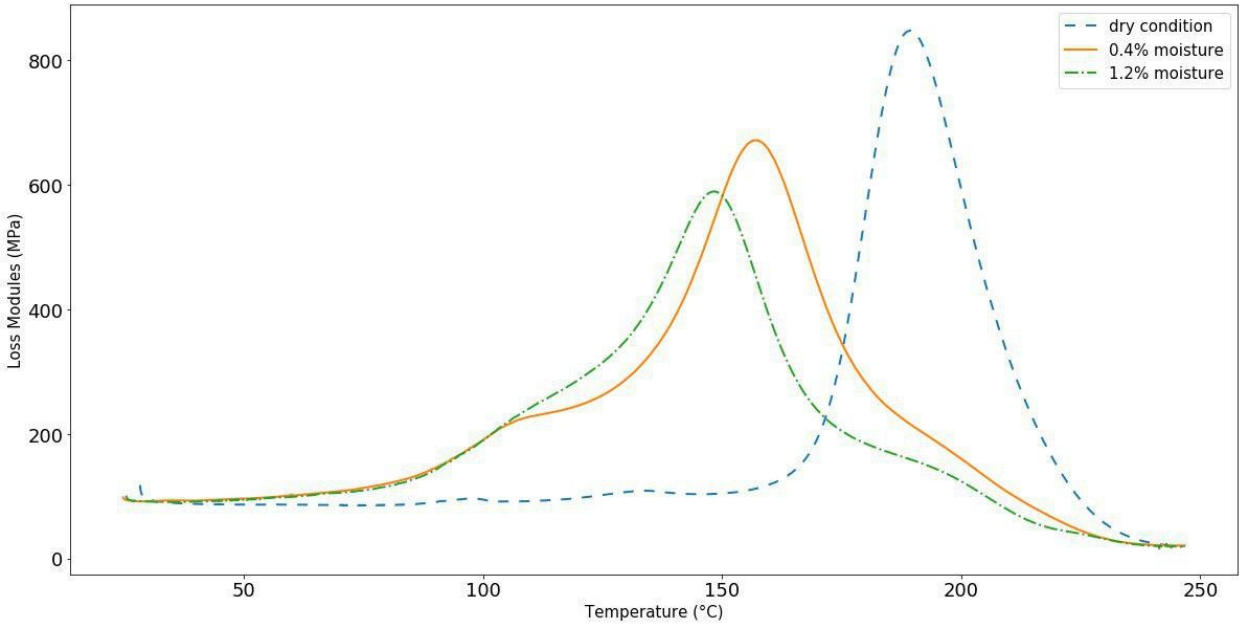

Figure 4-22 variation of loss modulus of UD samples with 1% void content for all levels of moisture in 90˚ direction

4.4.2.3 Effect of moisture on damping factor (tan δ)

Figure 4-23 demonstrates the effect of moisture on tan δ for laminates with 1% void content. It is apparent from the graph that the peak of tan δ decreased dramatically by about 43% after absorbing 0.4 % moisture. At the end, 51% reduction in loss modulus was reported after the absorption of 1.2% moisture.

4.4.2.4 Effect of moisture on glass transition temperature

The temperatures at which tan δ reached a maximum are known as T_g. *Figure 4-24* shows the variation of T_g as the amount of absorbed moisture increased. Like damping factor, Tg dropped from 201 ˚C to 166 ˚C after absorbing 0.4% moisture. Reduction in T_g was continuous as the laminate absorbed more moisture. Finally, T_g decreased to 154 ˚C when the laminate absorbed 1.2% moisture. The decrease in Tg was observed to be 23% less than that of the dry condition.

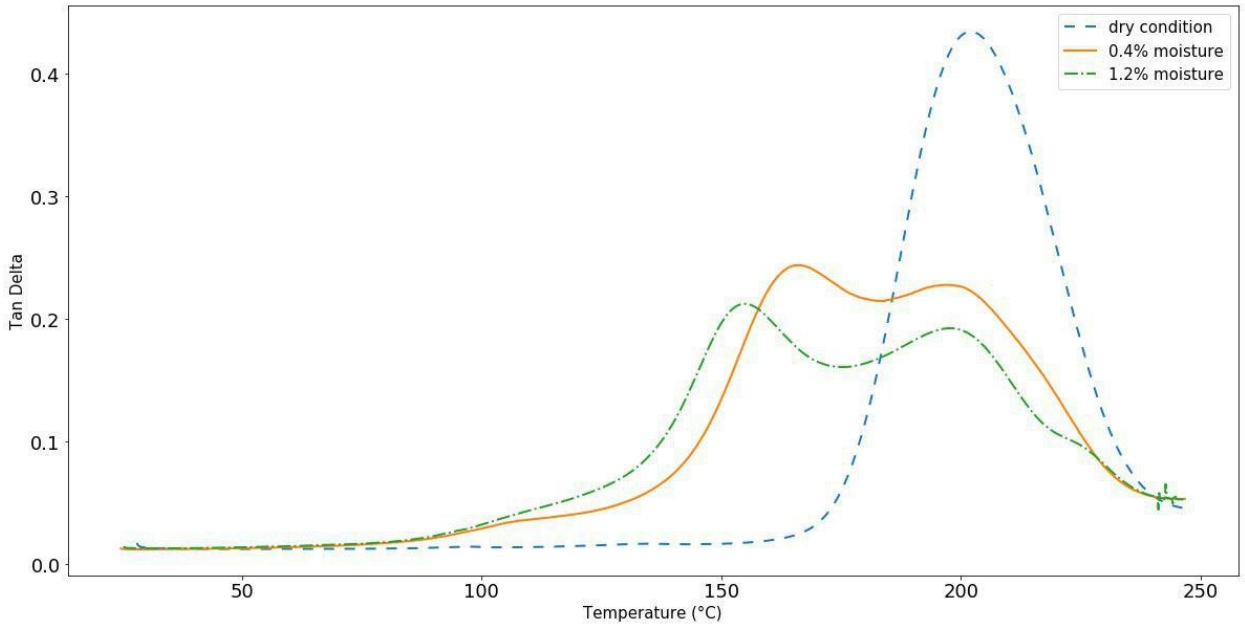

Figure 4-23 variation of Tan δ for UD samples with 1% void content at 90˚ direction with increase in amount of absorbed moisture

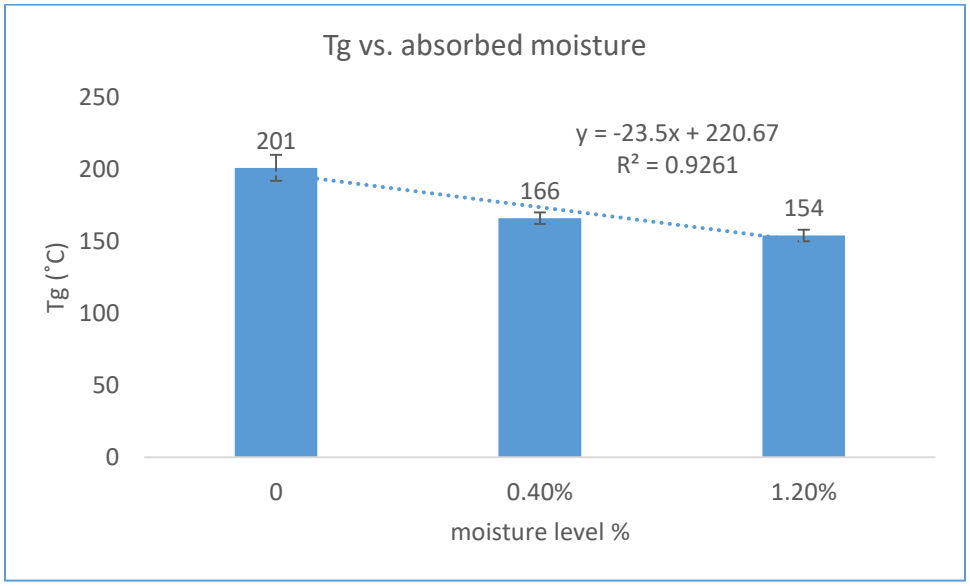

Figure 4-24 change of glass transition temperature with increase in amount of absorbed moisture for UD samples with 1% void content

4.4.3 Samples with 2% void content

Dynamic mechanical analysis had been done to monitor the variation of storage modulus, loss modulus, tan δ, and glass transition temperature. All the reported data are the average of two samples.

DMA was conducted on UD carbon/epoxy laminates with 2% void content and the results are provided in *Figure 4-25*. Variations of storage modulus, loss modulus, tan δ, and T_g as a function of temperature are shown below for the range of room temperature to 250 ˚C. The storage modulus of the samples tends to reduce as temperature increase because the laminate is changing from solid state to rubbery state. There is a sharp drop in storage modulus at the glass transition temperature. Like other samples with different void contents, loss modulus and tan δ increased as temperature increased and reached a peak value, which was again followed by a sharp decrease.

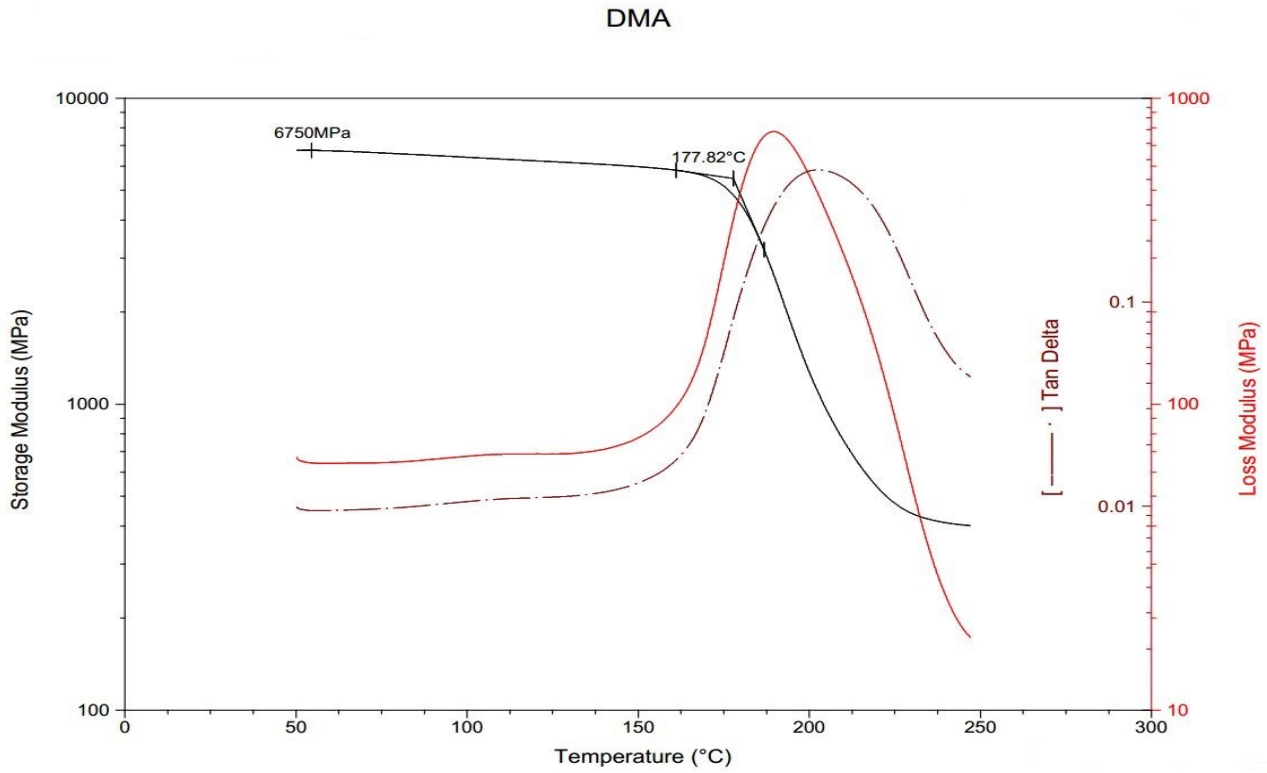

Figure 4-25 Dynamic mechanical analysis of UD samples with 1% void content vs temperature at Dry condition

4.4.3.1 Effect of moisture on storage modulus

Figure 4-26 shows the effect of moisture absorption on storage modulus of composite laminates with 2% void content. Although for previous samples, at lower void content, E′ inclined to reduce after absorbing moisture, but the trend was not the same for the current samples. Nevertheless, reduction in T_g is still visible from the graph.

To have a better understanding, Figure 4-27 indicates the storage modulus of samples at room temperature. It can be seen that storage modulus remained almost constant after absorbing 0.4%

moisture at 6750 MPa. Strangely, at the next moisture level, storage modulus increased and remained constant around 7100 MPa. The author believes, having non uniform void content at two first levels of moisture is affecting the experimental results in this graph.

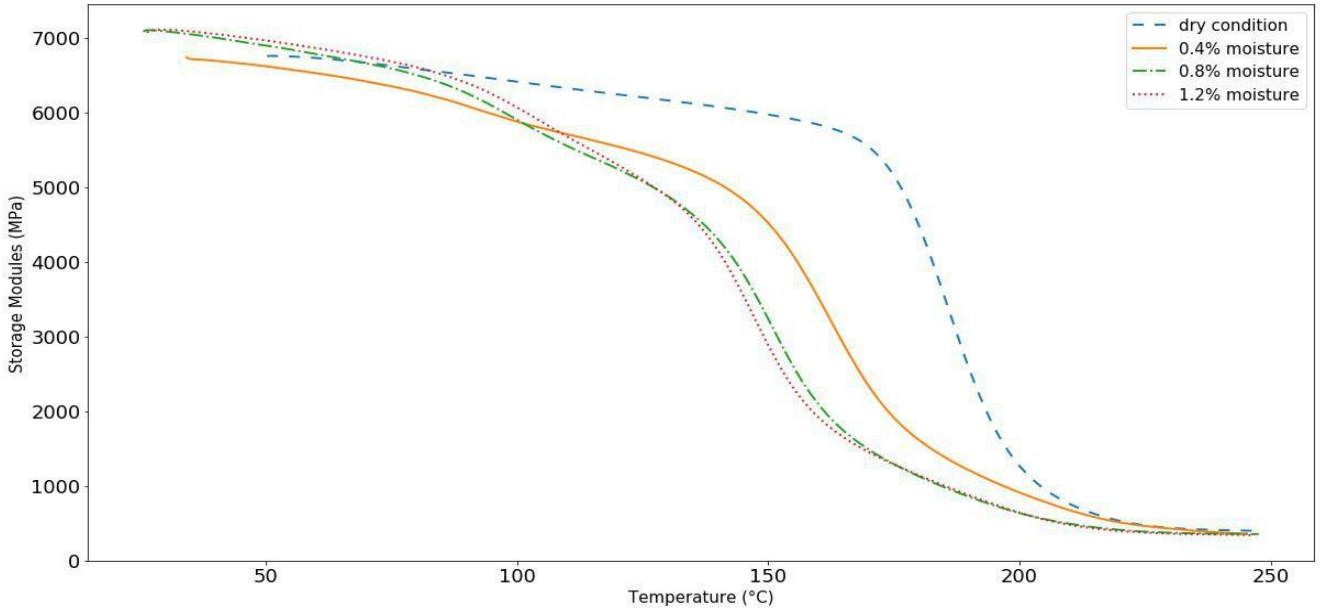

Figure 4-26 moisture effect on storage modulus of UD samples with 2% void content vs temperature at 90 ˚ direction

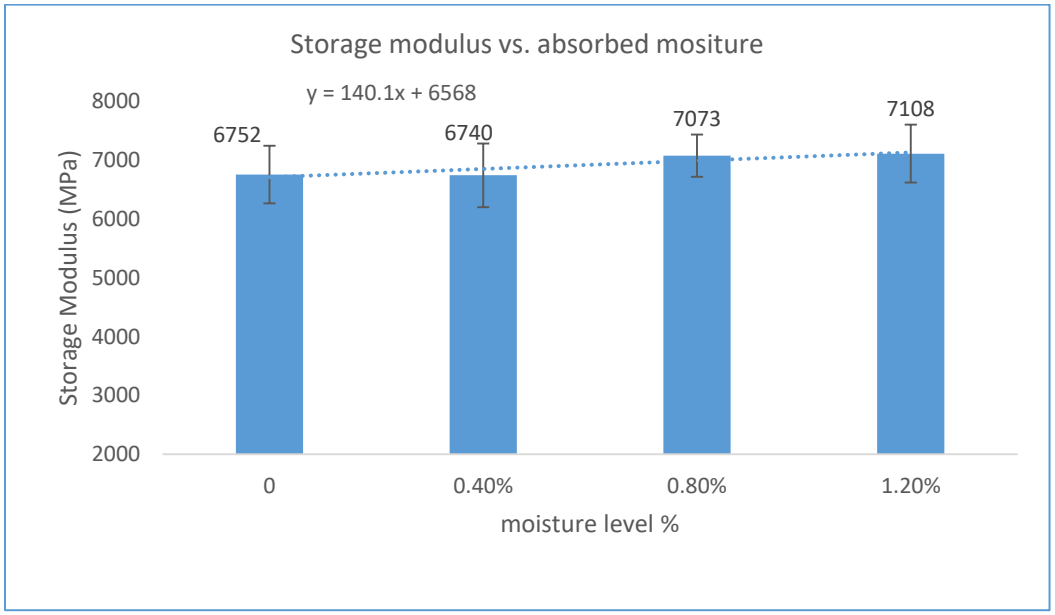

Figure 4-27 change of storage modulus of UD samples with 2% void content at 90 ˚ at room temperature for different levels of moisture

4.4.3.2 Effect of moisture on loss modulus

Figure 4-28 shows the variation of loss modulus as amount of absorbed moisture increased. It can be seen that loss modulus sharply decreased, from 777 MPa to 557 MPa, after absorbing 0.4% moisture while it increased slightly at next moisture levels and reached 604 MPa at the end.

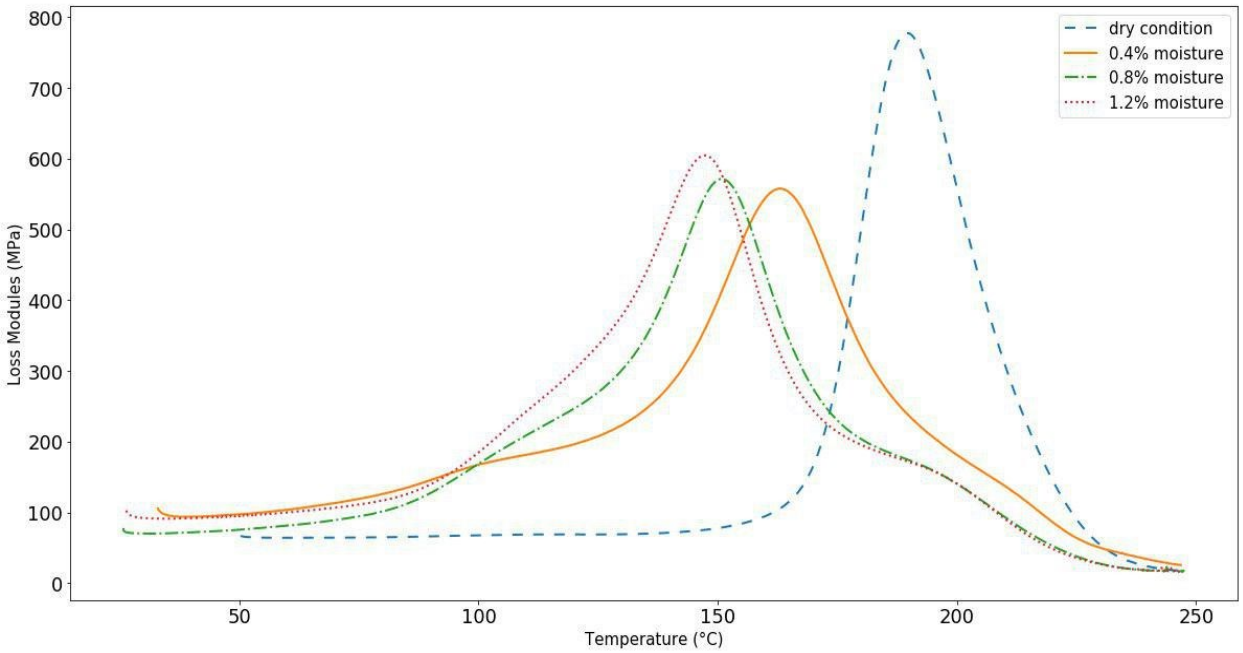

Figure 4-28 variation of loss modulus of UD samples with 2% void content for all levels of moisture in 90˚ direction

4.4.3.3 Effect of moisture on tan δ

Effects of moisture on tan δ for UD carbon/epoxy laminates are shown in Figure 4-29. Reviewing the peak values, it can be seen that the maximum value of tan δ decreased by about 50% after absorbing 0.4% moisture and it remained almost constant at the next moisture levels.

4.4.3.4 Effect of moisture on glass transition temperature

Figure 4-30 shows the effect of absorbed moisture on T_g of laminates containing 2% void content. As it can be seen, T_g continuously reduced as samples absorbed more moisture. For UD laminates, 23% drop in glass transition temperature was reported after absorbing 1.2% moisture.

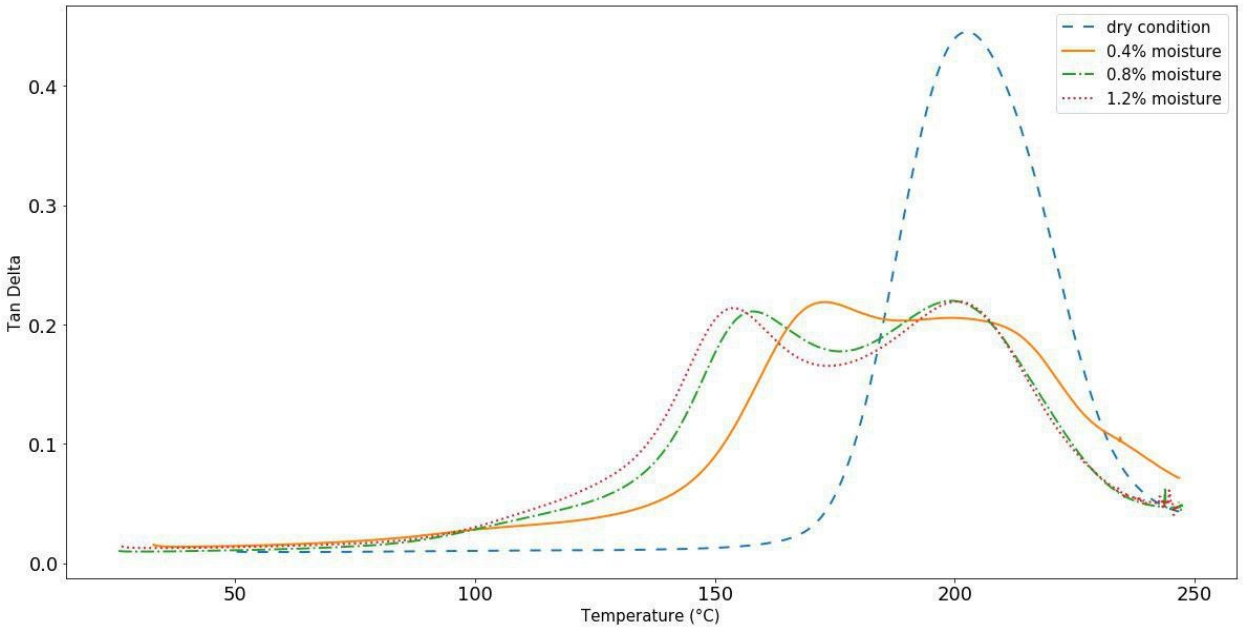

Figure 4-29 variation of Tan δ for UD samples with 2% void content at 90˚ direction with increase in amount of absorbed moisture

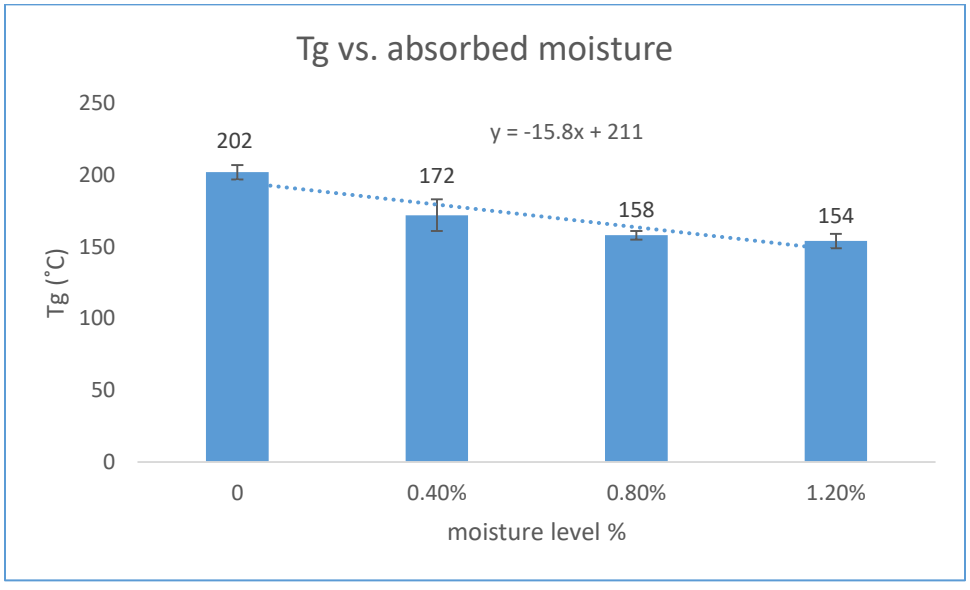

Figure 4-30 change of glass transition temperature with increase in amount of absorbed moisture for UD samples with 2% void content

4.6 Finite element analysis (FEA)

Developing a finite element model has been proven to solve an engineer's difficulties especially in terms of time and error reduction in the last few decades. Nowadays, finite element analysis has become a very powerful tool for the analysis of complex geometries. Prediction of behaviour of different industrial parts under one or several conditions (mixed or one at a time) has become one of the most useful applications of FEA in today's research groups and industries. As an example, to study the moisture absorption procedure in composite laminates experimentally, the samples should be kept immersed in water for almost one year as mentioned in previous sections. While using FEA tools, the mass diffusion process can be simulated in order of few minutes. The purpose of doing FEA is to simulate the moisture absorption curve for each level of void content and compare the results with our experimental graphs. Thus, to observe the differences in moisture absorption of samples at different void content levels, mass diffusion module of ABAQUS software was used to compare the change of mass concentration of moisture in all samples with time. Another study was conducted to predict the moisture profile growth in the laminate at micro level in the presence of fibers.

4.6.1 FEA modeling

Two different scales of FEA were modeled to study the moisture absorption procedure for CFRP laminates. At macro level, three 2D homogenous laminates were modeled according to the original dimensions of laminates while at micro level, a 2D model was performed to see how moisture passes through the fiber bundles.

4.6.1.1 Macro model

In previous sections, it was observed that a difference in void content can lead to a difference in diffusivity. Three 2D models were built with the assumption of different diffusion coefficient for each level of void content. Sample dimensions and properties are summarized in Table 4-5 below:

Table 4-5 summerizing the model properties in ABAQUS software

Void content	Dimension	Moisture equilibrium	Diffusion coefficient (D_x) (E-7 mm^2/s)
0.2%	100 mm × 3.4 mm	1.69 %	1.16
1%	100 mm × 3.5 mm	1.74 %	1.20
2%	100 mm × 3.9 mm	1.93 %	1.24

Figure 4-31 indicates the 2D design of the laminate using the ABAQUS software. The schematic design is very similar for all three types of samples; however, only the void free sample is presented below:

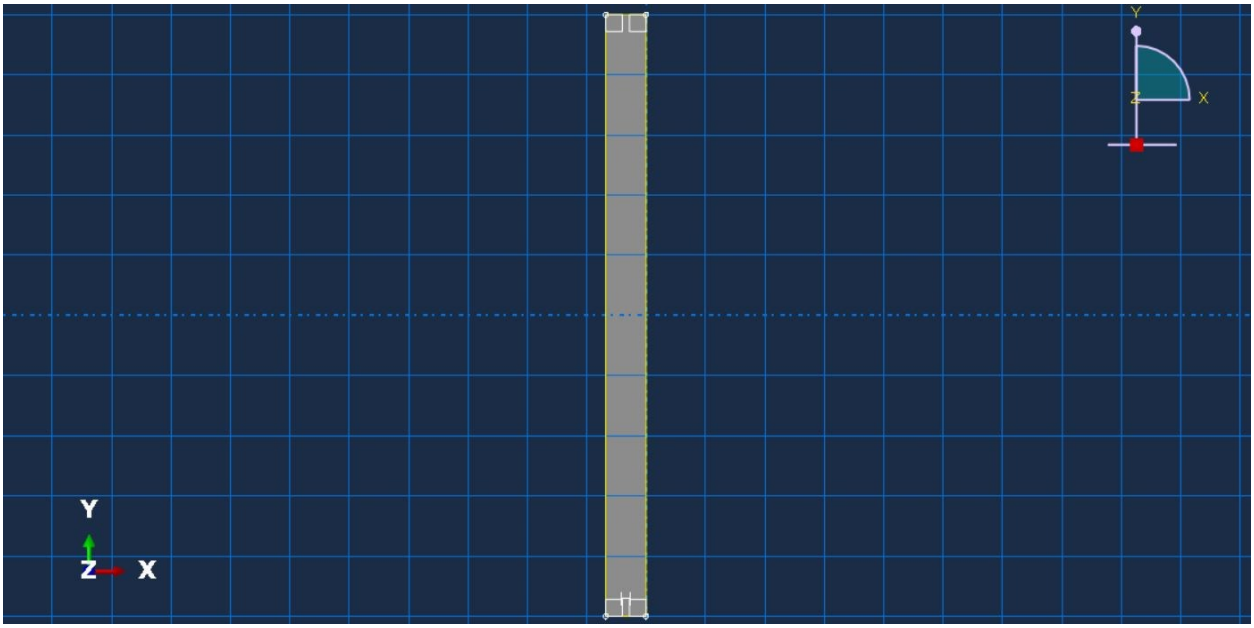

Figure 4-31 a schematic view of 2D design of the CFRP laminate to model the moisture absorption

4.6.1.1.1 Formulation and modeling strategy

For modeling the mass diffusion process, the ABAQUS program was used. To simulate the mass diffusion, ABAQUS uses an extended form of the Fick's law equation, which is capable of modeling a non-uniform solubility of the solute in the base material and also considers the temperature and pressure gradients in the process [65-67].

ABAQUS software uses normalized concentration as a function of solubility of the diffusing material. Normalized concentration is defined as follows:

$$\varphi = c/s \tag{12}$$

Where:

c is the mass concentration $[\frac{g}{mm^{-3}}]$,

s is the solubility of the solute $[s^2 mm^{-2}]$

Reason of this type of definition is that normalized concentration can be continuous at the interface of different material while using regular concentration can lead to discontinuity at the interface in the base material. In our study, we modeled the mass diffusion of moisture (solute) to the CFRP laminate (base material). So, due to the fact that the laminate does not have any dissimilar material, the solubility was considered as unity and in our case mass concentration and normalized concentration are the same.

4.6.1.1.2 Boundary conditions

Considering that the samples were bound to aluminium on all four sides along the thickness, no boundary condition was applied to the edges knowing that the software considers the edges without boundary conditions as being insulated and moisture cannot diffuse through these edges. On the other hand, mass diffusion boundary condition with the amplitude of maximum saturation level was applied on the two other surfaces. The schematic of boundary conditions is provided at Figure 4-32.

4.6.1.2 Micro model

To observe the moisture profile along the fibers, a micro level FEA was conducted. The model dimension was 0.127 mm × 0.05 mm, where 0.127 mm was considered as the thickness of each ply. Fibers were considered non-permeable and circular with diameter of 7 μm. Fiber volume fraction was calculated as 62% using hexagonal fiber arrangement [68]. Moisture equilibrium and diffusivity of the sample was considered the same with void free samples. Figure 4-33 indicates the 2D model at micro level.

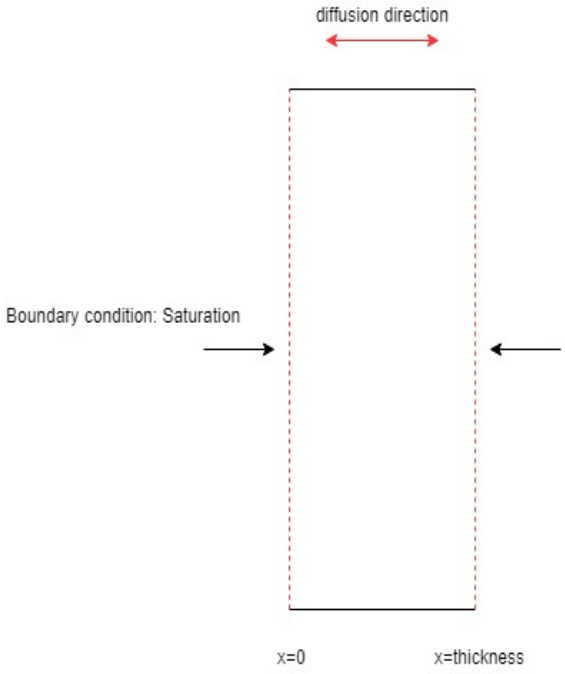

Figure 4-32 a schematic of applied boundary condition in ABAQUS to simulate the moisture diffusion through the thickness of the laminate

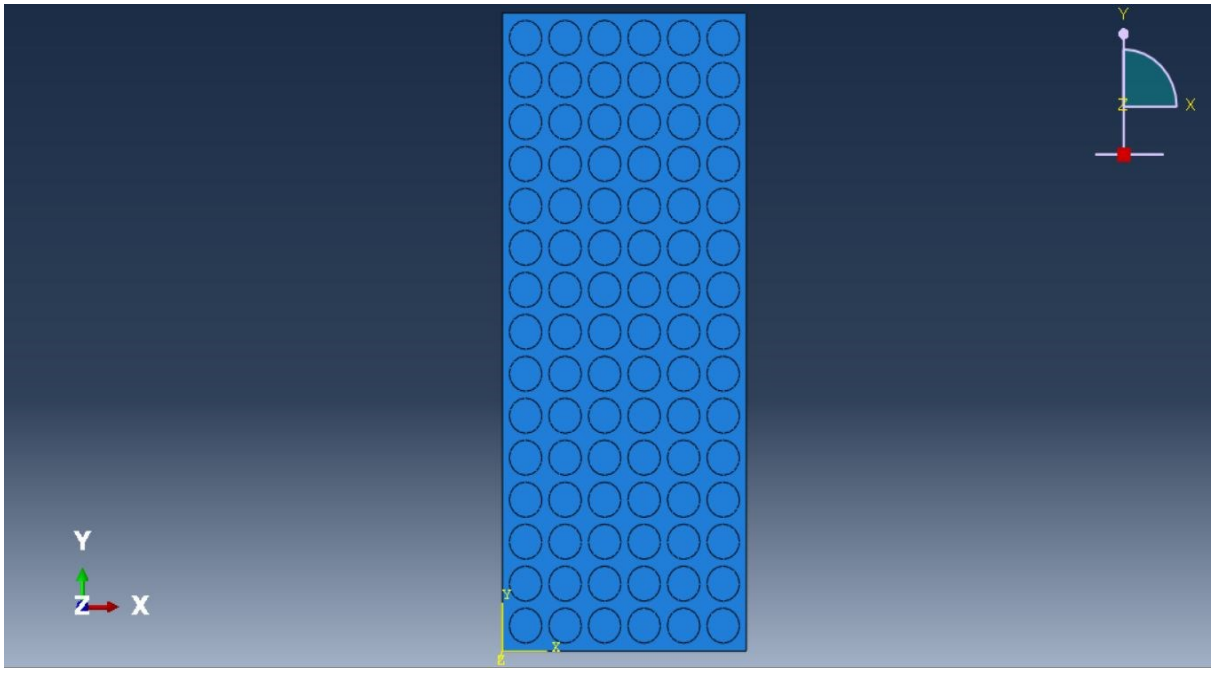

Figure 4-33 a 2D model at micro model to simulate the moisture diffusion through the fibers

4.6.1.2.1 Boundary conditions

To observe how moisture can diffuse between the fibers, moisture was applied from the bottom side of the sample and all other edges were considered as insulated. Figure 4-34 indicates the applied boundary condition for the FEA at micro level.

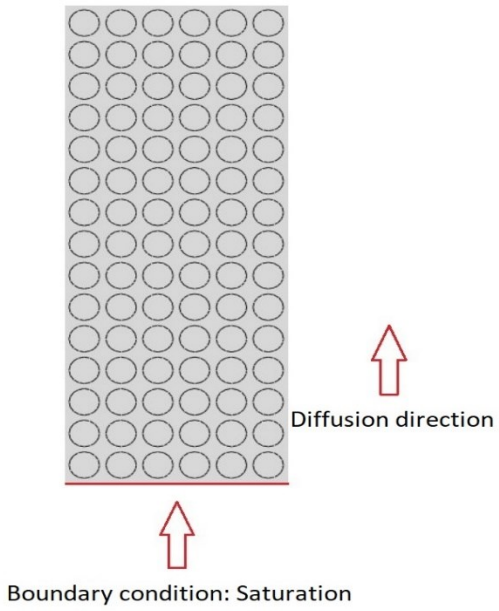

Figure 4-34 applied boundary condition at the bottom of the ply

4.6.2 Meshing

Mesh convergence study was conducted for both models at micro and macro level. During FEA, when two different runs with different mesh sizes lead to the same or very close results, it is recommended to stop mesh size reduction for reducing the calculation time and computational facilities. As it can be seen in Figure 4-35, the mass concentration through the thickness of the material was studied for four different mesh sizes, however it was decided to choose 0.1 mm as mesh size for this study after studying the mesh sensitivity. For the macro model, the quadrilateral meshes (DC2D4 with A 4-node linear heat transfer quadrilateral element type) were generated. Also, for the micro model, the triangular element shapes (DC2D3: with A 3-node linear heat transfer triangle element type) were used.

After doing the mesh sensitivity analysis for the micro modeling, 0.3 µm mesh size was selected for the micro models to optimize the required time and computational quality. Figure 4-36 indicates the final mesh generation for both models.

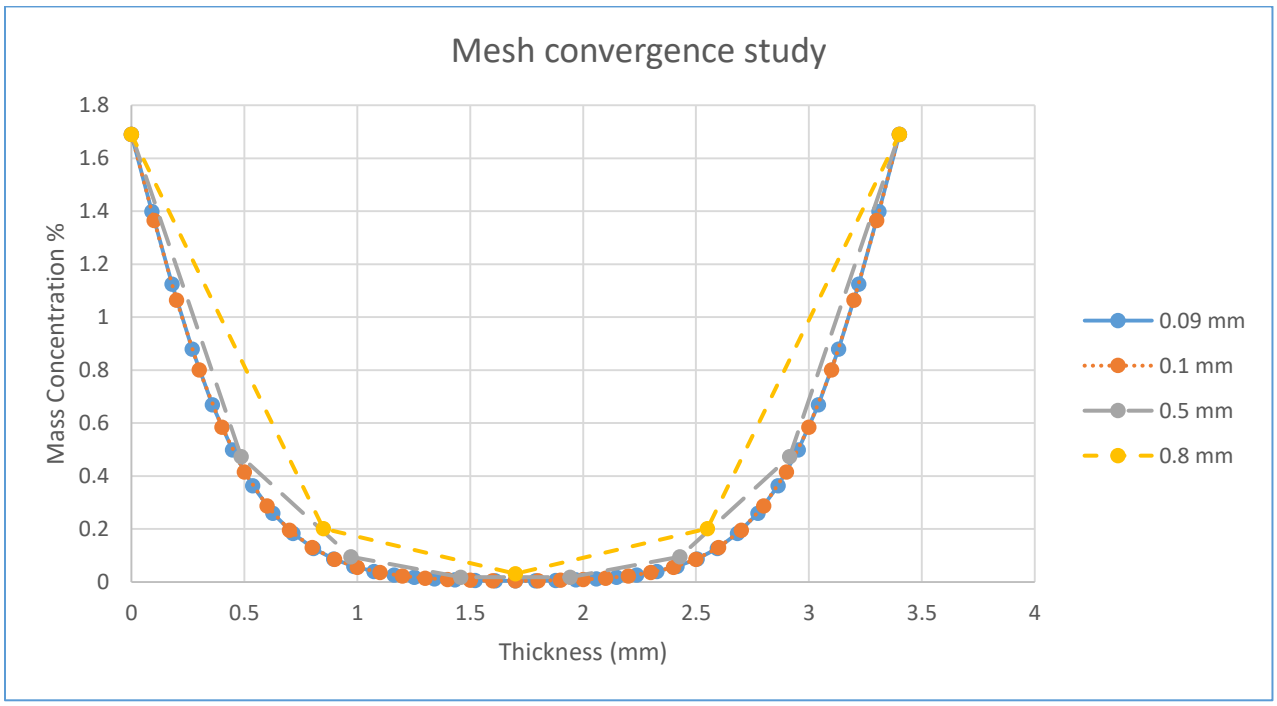

Figure 4-35 Mesh convergence study for the laminate with 0.2% void content at 10 days exposure time

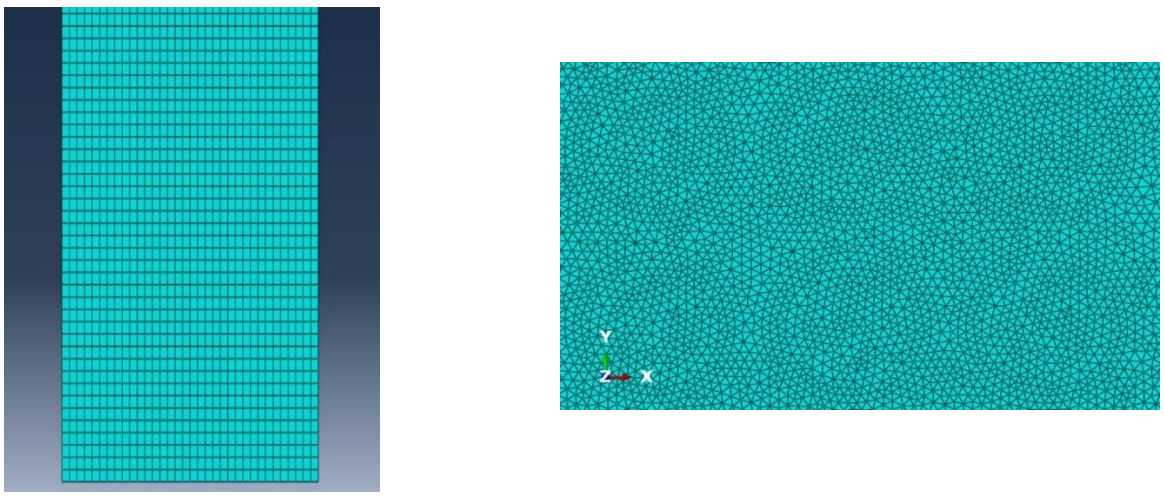

Figure 4-36 meshing process at macro and micro models

4.7 Finite element analysis results

4.7.1 Macro model analysis

Several 2D models were employed to observe the moisture concentration distribution along the thickness of the laminates at three different levels of void content. Each sample was exposed to the saturation level for 30, 90, and 365 days. At each exposure time, change of mass concentration through the thickness of the laminate was observed and compared for all three kinds of laminates. Due to the difference in thickness for each level of void content, the normalized thickness was taken into account to make the graph more visible.

As it can be seen, the CONC output from ABAQUS software provides useful information about the mass diffusion of moisture through the thickness of CFRP laminates. For all three time increments, adjacent plies to the boundary condition reach the maximum moisture level rapidly. As the distance of the plies from the boundary condition increases, the amount of moisture decreases and reaches to its minimum at the mid-plane. Difference in maximum and minimum amount of mass concentration increased as void content increased in the modeled laminate. This can explain why moisture diffusion process takes longer as void content increases.

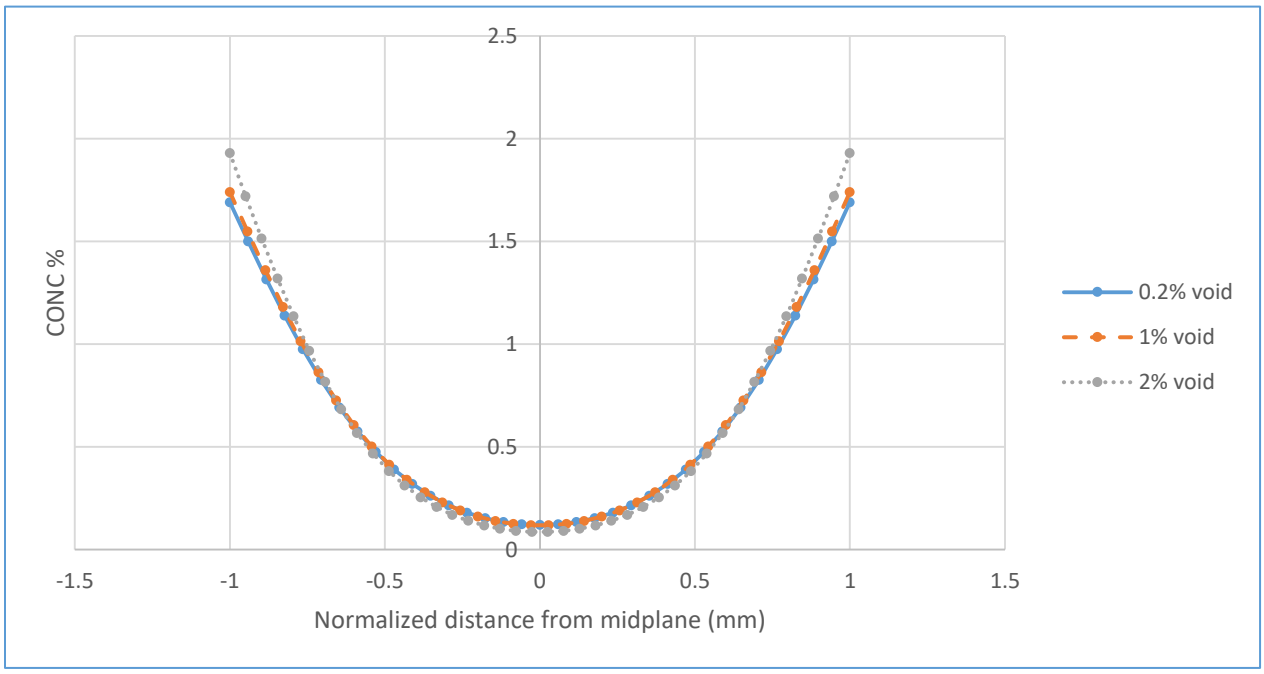

Figure 4-37 moisture concentration through the thickness of laminates at different levels of void contents after 30 days exposing to moisture environment

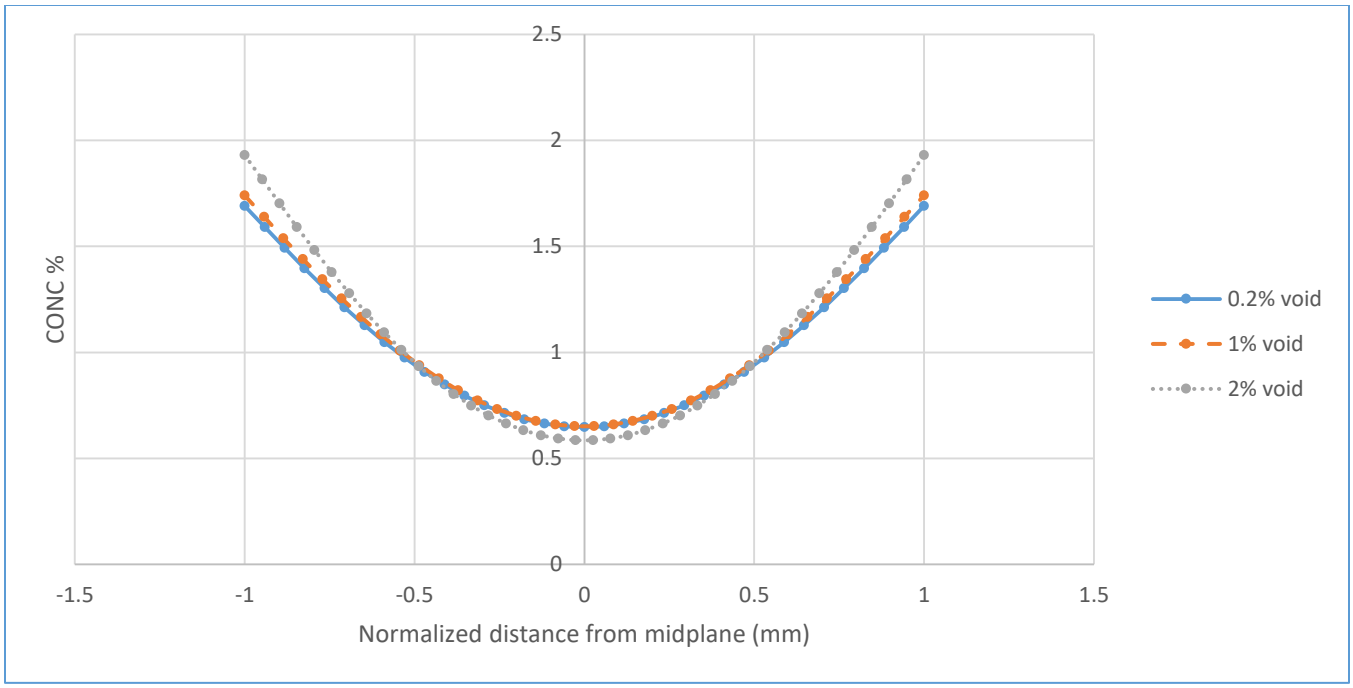

Figure 4-38 moisture concentration through the thickness of laminates at different levels of void contents after 90 days exposing to moisture environment

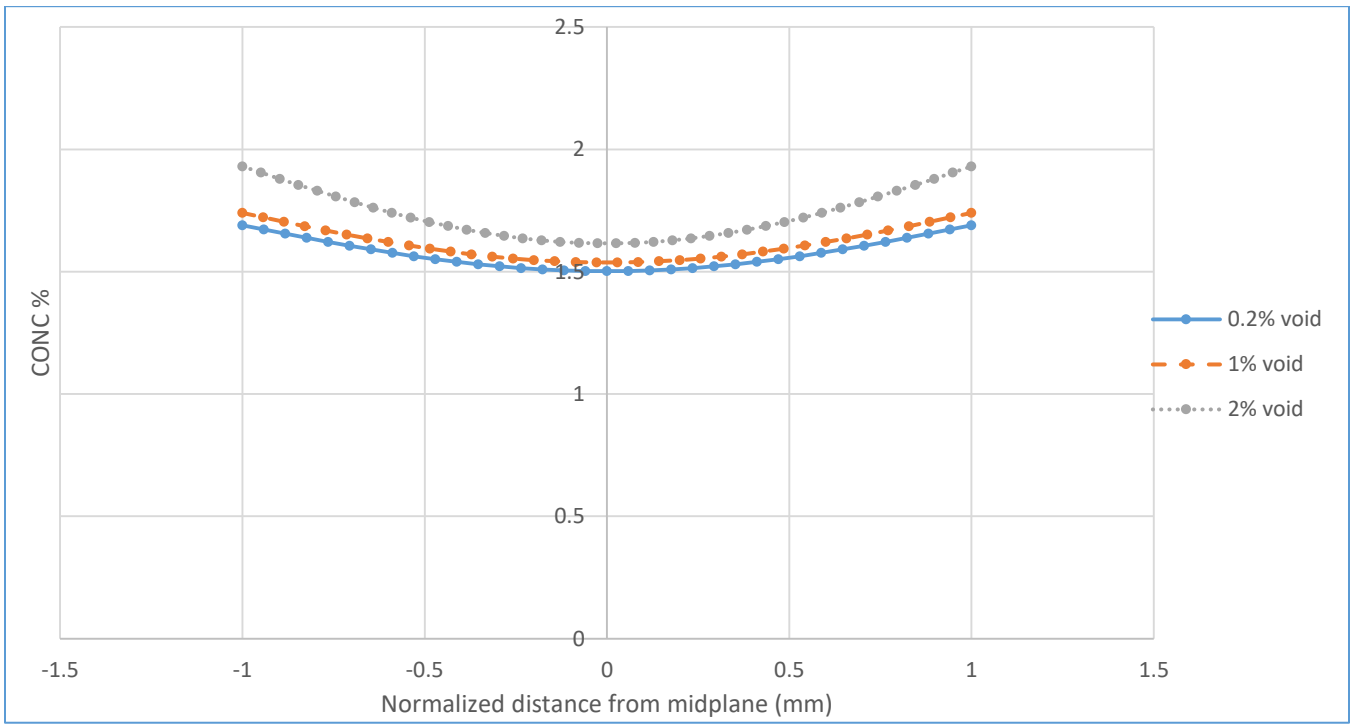

Figure 4-39 moisture concentration through the thickness of laminates at different levels of void contents after 365 days exposing to moisture environment

Considering the equation 3, the total gained weight of the material resulting from absorbing moisture can be calculated by integrating the equation 3 over the thickness of the laminate at different exposure times [69].

$$m = \int_0^h c \, dx \tag{13}$$

Using equation 13, the mass gain related to the moisture was calculated. However, after calculating the simulated weight of moisture, the author could not verify the simulation results with the experiments due to existing a large difference in experimental and simulation results.

4.7.2 Micro model analysis

A micro level study was conducted to observe the moisture diffusion between fibers. Figure 4-40 shows the moisture profile among the fiber arrangements after 24 hours exposure time. The areas closer to the boundary condition reached to the maximum level of moisture as it was expected. The moisture profile tended to go along y direction rather than x direction while the space behind the fibers absorbed less amount of moisture.

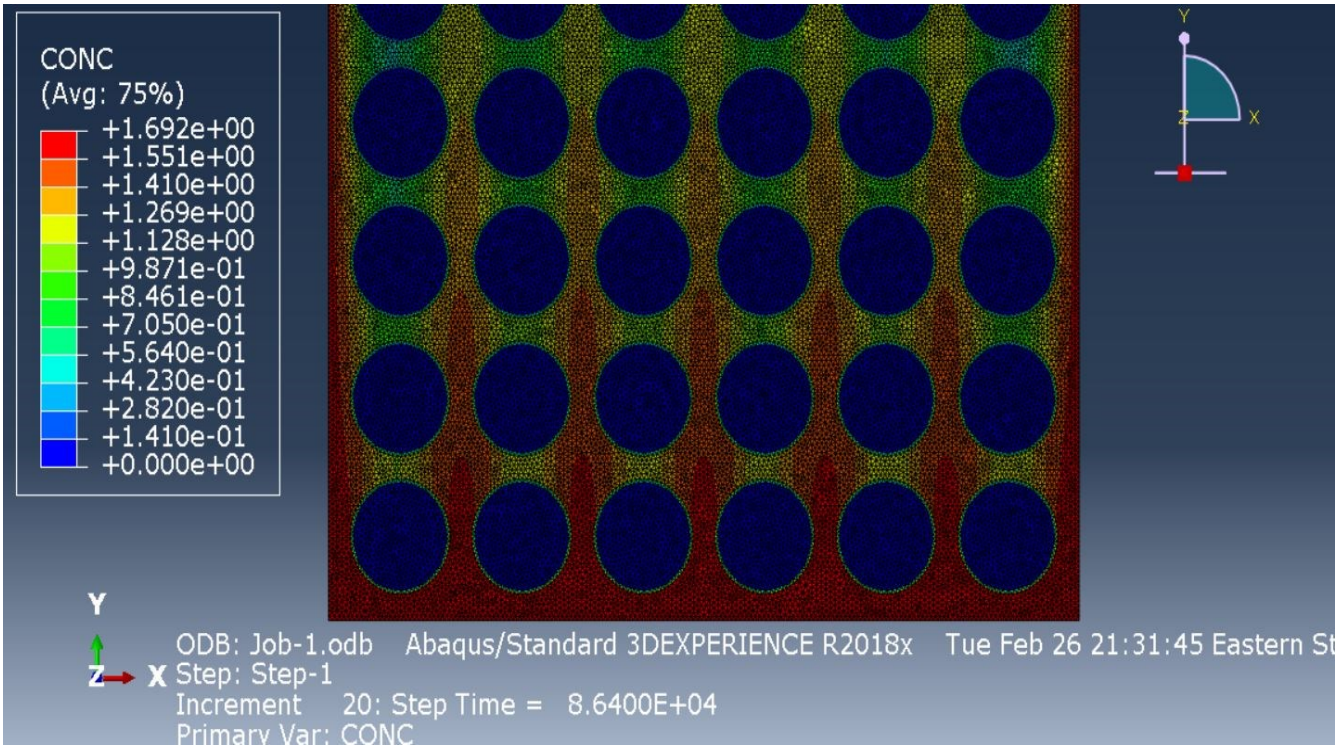

Figure 4-40 moisture diffusion profile between the fibers

Chapter 5

5 Conclusion and Future Work

5.1 Conclusion

In this research, the moisture absorption of carbon/epoxy unidirectional composite laminates, manufactured by out-of-autoclave technique, and the effects of moisture on their mechanical properties were studied. This research was conducted on three unidirectional composite laminates containing different levels of void content exposed to moisture at 60 ˚C. Moisture absorption behaviour of the laminates were studied using Fick's law of diffusion. Moreover, several mechanical tests were conducted at dry condition and after absorption of 0.4%, 0.8%, and 1.2% moisture and the results were monitored and compared. It was found that changes in mechanical behaviour of the laminates can be described by change in molecular chains in polymeric matrix and increasing the plasticization of the material due to presence of moisture molecules inside the laminates.

The specific results from all the experiments obtained from the current study are summarized as follows:

- Uniform void contents were formed in the composite laminates and the amount of void contents were increased as the applied vacuum pressure and the frequency of using a roller decreased.
- Moisture absorption of all laminates was monitored. The initial slope of the curve remained constant up to almost 75% of the maximum level of absorbed moisture for all levels of void content. It was found that as the amount of void content increased, the amount of absorbed moisture also increased. Studying the effect of void content on moisture diffusivity of the material through its thickness was another objective of this research. It was shown that as the void content of the sample increased, the diffusivity of the material also increased. A linear equation was also suggested to relate void content of the laminates and diffusivity.

- Interlaminar shear strength (ILSS) of the laminates were studied by short beam shear tests at three-point bending mode. The moisture effects on ILSS was almost the same for all levels of void content. The ILSS of the UD laminates were not affected by moisture until 0.4% moisture level was attained. After this level, moisture reduced the ILSS drastically by about 15% compared to the dry condition. Moreover, the joint effect of moisture and void content on ILSS was presented.
- Viscoelastic response of the laminates under sinusoidal loading were monitored by performing dynamic mechanical analysis. The effects of moisture on storage modulus was almost the same as the ILSS. By increasing the amount of moisture, storage modulus of the samples with 0.2% and 1% void content decreased while some fluctuations for the samples at 2% void content were observed.
- Glass transition temperatures (T_g) for all the laminates were determined by the temperatures related to the peak value of tan δ graph from DMA experiments. It was found that moisture generally reduced the glass transition temperature of the laminates. T_g tended to reduce drastically after each moisture absorption level. In all levels of void content, T_g reduced by almost 25% after absorbing 1.2% moisture, compared to the dry condition. The main effect of moisture on loss modulus was observed after first moisturising period. For all laminates, after absorbing 0.4% moisture, loss modulus dropped drastically and remained almost constant afterwards.
- A finite element analysis was conducted at micro and macro levels. A macro modeling was used to observe the change of mass concentration through the thickness of the material at different exposure times. It was observed that the plies near the boundary conditions reached the maximum level of moisture rapidly while the mass concentration at the mid-plane was always minimum for all the models. Moreover, it was found that difference in maximum and minimum amount of mass concentration increased as void content increased. A micro modeling was used to simulate moisture diffusion through the fiber bundles. After one day exposure time, it was found that moisture did not tend to go to the space between the fibers along y direction.

5.2 Contribution

In this study, the effects of moisture on properties of carbon fiber laminates at different void levels was studied. The samples were manufactured using OOA technique and the amount of void content had been verified by doing microscopic observation. Moisture absorption of the samples was tracked at a moisturising pot at 60 ˚C for more than one year at three levels of void content. Interlaminar shear strength and dynamic mechanical analysis were conducted to observe the moisture effects on mechanical properties of the laminates. After observing the moisture absorption curves for all void levels, diffusivity of the material in all void levels were calculated and a mathematical model was suggested to relate the void content and diffusivity. The modified DeBenedetto equation was suggested to estimate the glass transition temperature of the laminate at all moisture levels.

Summarized format of our contribution are as follow:

- A manufacturing method was followed to make three different carbon fiber laminates with different levels of void content.
- Microscopic observation was done to verify the void level of the samples
- Moisture absorption behaviour of the laminates at all levels of void contents were studied and the diffusivity of the materials was calculated after one year of immersion
- Viscoelastic behaviour of the laminates was studied by conduction DMA tests. Moisture effects on the stiffness of the material and glass transition temperature was reported. The modified DeBenedetto equation was suggested to relate the glass transition temperature of the material at all moisture levels.
- Shear strength of the laminates was studied by doing ILSS tests to observe the moisture effects on matrix properties.

5.3 Future work

Moisture absorption of carbon/epoxy laminates and its effects on the mechanical properties of the laminates at different levels of moisture have been studied.

To have a more realistic simulation in space applications, it is necessary to study the cyclic moisture absorption and its effects on the mechanical properties. Adding different thermal and cooling cycles (because of rain, snow and temperature differences in a day) can represent the real condition in a better way. In this study, only UD laminates have been studied, but different stacking sequences should be studied to find a correlation between the fiber orientation, thickness of the material, and the water resistance capacity of the material.

In this study, the moisture diffusion through the thickness of the material was studied. It is suggested to find the diffusion coefficients in all directions and study the effects of fiber orientation and stacking sequences on diffusivities. Moreover, the moisture diffusion process can be done in different temperatures to study the effects of crosslinking in the moisture absorption process and mechanical properties of the material after exposure to moisture.

Furthermore, external loadings combined with moisture diffusion can be added to the FEA to compare the FEM results to the experimental results from this thesis.

Publication – Conference

- Afshin Bayatpour, Mehdi Hojjati, “Moisture Effect on Mechanical Performance of Out-of-Autoclave Composite Material at Different Void Level” CSME-CFDSC Congress June 2-5, 2019, London, On, Canada
- Afshin Bayatpour, Mehdi Hojjati, “Laminate Through-The-Thickness Moisture Diffusion Coefficient at Different Void Contents” CASI AERO Conference May14-16, 2019, Laval, QC, Canada

Reference

1. Soutis, C., *Carbon fiber reinforced plastics in aircraft construction.* Materials Science and Engineering: A, 2005. **412**(1-2): p. 171-176.
2. Soutis, C., *Fibre reinforced composites in aircraft construction.* Progress in Aerospace Sciences, 2005. **41**(2): p. 143-151.
3. Cobra, J. *Aircraft Structural Components*. 2010; Available from: http://aircraftscomponents.blogspot.com/2012/08/aircraft-structural-components.html.
4. one, C. *Industry: Marine*. 2019; Available from: https://www.compositesone.com/product/industries/marine/.
5. *The Space Environment*. Available: https://www.faa.gov/other_visit/aviation_industry/designees_delegations/designee_types/ame/media/Section%20III.4.1.2%20The%20Space%20Environment.pdf.
6. Nugroho, A.M.J.J.o.E. and Engineering, *A preliminary study of thermal environment in Malaysia's terraced houses.* Journal of Economics and Engineering, 2011. **2**(1): p. 25-28.
7. Bureau, A., *How old is too old? The impact of aging aircraft on flight safety.* Australian Transport Safety Bureau, 2007: p. 221-236.
8. Robinson Helicopter Company, Model R22 Mariner, Bents Basin State Recreation Area, NSW, 20 June 2003. Aviation Safety Investigation Report. No: 200302820. Canberra: Australian Transport Safety Bureau (ATSB); 2005.
9. Wong, K.J., *Moisture absorption characteristics and effects on mechanical behaviour of carbon/epoxy composite: Application to bonded patch repairs of composite structures*. 2013, Dijon.
10. Myung Cheon, L. and N.A. Peppas, *Water transport in epoxy resins.* Progress in Polymer Science, 1993. **18**(5): p. 947-961.

11. Meares, P., *Polymers: structure and bulk properties*. 1965: Van Nostrand Reinhold.

12. Diamant, Y., G. Marom, and L.J. Broutman, *The effect of network structure on moisture absorption of epoxy resins.* Journal of Applied Polymer Science, 1981. **26**(9): p. 3015-3025.

13. Vanlandingham, M.R., R.F. Eduljee, and J.W. Gillespie, *Moisture diffusion in epoxy systems.* Journal of Applied Polymer Science, 1999. **71**(5): p. 787-798.

14. Moy, P. and F.E. Karasz, *Epoxy-water interactions.* Polymer Engineering and Science, 1980. **20**(4): p. 315-319.

15. George, S.C. and S. Thomas, *Transport phenomena through polymeric systems.* Progress in Polymer Science, 2001. **26**(6): p. 985-1017.

16. Prager, S., E. Bagley, and F.A. Long, *Diffusion of Hydrocarbon Vapors into Polyiso-butylene. II1.* Journal of the American Chemical Society, 1953. **75**(5): p. 1255-1256.

17. Fujita, H., A. Kishimoto, and K. Matsumoto, *Concentration and temperature dependence of diffusion coefficients for systems polymethyl acrylate and n-alkyl acetates.* Transactions of the Faraday Society, 1960. **56**: p. 424-437.

18. Frisch, H.L., *"Diffusion in polymers" edited by J. Crank and G. S. Park, Academic Press, London and New York, 1968; 452 pg.* Journal of Applied Polymer Science, 1970. **14**(6): p. 1657-1657.

19. Manson, J.A. and E.H. Chiu, *Permeation of liquid water in a filled epoxy resin.* Journal of Polymer Science: Polymer Symposia, 2007. **41**(1): p. 95-108.

20. Kwei, T.K. and C.A. Kunins, *Polymer–filler interaction: Vapor sorption studies.* Journal of Applied Polymer Science, 1964. **8**(3): p. 1483-1490.

21. Varghese, S., et al., *Effect of Adhesion on the Equilibrium Swelling of Short Sisal Fiber Reinforced Natural Rubber Composites.* Rubber Chemistry and Technology, 1995. **68**(1): p. 37-49.

22. Das, B., *Restricted equilibrium swelling—A true measure of adhesion between short fibers and rubber.* Journal of Applied Polymer Science, 1973. **17**(4): p. 1019-1030.

23. Pogany, G.A., *Anomalous diffusion of water in glassy polymers.* Polymer, 1976. **17**(8): p. 690-694.

24. Gillat, O. and L.J. Broutman, *Effect of an External Stress on Moisture Diffusion and Degradation in a Graphite-Reinforced Epoxy Laminate*, in *Advanced Composite Materials—Environmental Effects*. 1978, ASTM International. p. 61-61-23.

25. Lv, X.J., et al., *Study of the Influence of Immersion on the Carbon Fiber/Epoxy Composites.* Journal of Reinforced Plastics and Composites, 2008. **27**(6): p. 659-666.

26. Fick, A.J.A.d.P., *Ueber diffusion.* 1855. **170**(1): p. 59-86.

27. Jost, W.J.L., Gases, *Diffusion in solids.* 1960. **73**.

28. ASTM, D. *5229/D 5229M: Standard test method for moisture absorption properties and equilibrium conditioning of polymer matrix composite materials*. 2004. American Society For Testing and Materials.

29. Shanker, A., R.W. Sullivan, and D.A. Drake, *Elastic Properties of CYCOM 5320-1/T650 at Elevated Temperatures Using Response Surface Methodology*, in *Composite, Hybrid, and Multifunctional Materials, Volume 4*. 2015, Springer. p. 29-37.

30. Jackson, K. and M. Crabtree. *Autoclave quality composites tooling for composite from vacuum bag only processing*. in *47 th International SAMPE Symposium and Exhibition 2002*. 2002. International SAMPE Symposium and Exhibition.

31. Dang, C., et al. *Mechanical Comparison of Outof-Autoclave Prepreg Part to Conventional Autoclave Prepreg Part'*. in *American Helicopter Society 67th Annual Forum*. 2011.

32. Centea, T., L.K. Grunenfelder, and S.R. Nutt, *A review of out-of-autoclave prepregs – Material properties, process phenomena, and manufacturing considerations.* Composites Part A: Applied Science and Manufacturing, 2015. **70**: p. 132-154.

33. Sutter, J.K., et al., *Comparison of autoclave and out-of-autoclave composites.* nasa technical reports server, 2010.

34. Abdel Wahab, M.M., et al., *Coupled stress-diffusion analysis for durability study in adhesively bonded joints.* International Journal of Adhesion and Adhesives, 2002. **22**(1): p. 61-73.

35. Ashcroft, I.A., M.M.A. Wahab, and A.D. Crocombe, *Predicting Degradation in Bonded Composite Joints Using a Semi-Coupled Finite-Element Method.* Mechanics of Advanced Materials and Structures, 2003. **10**(3): p. 227-248.

36. Mahdavi, S., *Thermal Cycling of Out-Of-Autoclave Thermosetting Composite Materials*. 2017, Concordia University.

37. ASTM, *Standard test method for short-beam strength of polymer matrix composite materials and their laminates.* 2000.

38. Bowles, K.J. and S. Frimpong, *Void Effects on the Interlaminar Shear Strength of Unidirectional Graphite-Fiber-Reinforced Composites.* Journal of Composite Materials, 2016. **26**(10): p. 1487-1509.

39. Joshi, O.K., *The effect of moisture on the shear properties of carbon fibre composites.* Composites, 1983. **14**(3): p. 196-200.

40. Wang, Z., et al., *Durability study on interlaminar shear behaviour of basalt-, glass- and carbon-fibre reinforced polymer (B/G/CFRP) bars in seawater sea sand concrete environment.* Construction and Building Materials, 2017. **156**: p. 985-1004.

41. Daniels, B.K., N.K. Harakas, and R.C. Jackson, *Short beam shear tests of graphite fiber composites.* Fibre Science and Technology, 1971. **3**(3): p. 187-208.

42. Pavlidou, S. and C.D. Papaspyrides, *The effect of hygrothermal history on water sorption and interlaminar shear strength of glass/polyester composites with different interfacial strength.* Composites Part A: Applied Science and Manufacturing, 2003. **34**(11): p. 1117-1124.

43. Viña, J., et al., *The effect of moisture on the tensile and interlaminar shear strengths of glass or carbon fiber reinforced PEI.* Journal of Materials Science Letters, 2000. **19**(7): p. 579-581.

44. Lahelin, M., et al., *DMA testing of Ni–Mn–Ga/polymer composites.* Composites Part A: Applied Science and Manufacturing, 2009. **40**(2): p. 125-129.

45. Aaltio, I., et al., *Temperature dependence of the damping properties of Ni–Mn–Ga alloys.* Materials Science and Engineering: A, 2008. **481-482**: p. 314-317.

46. Hassan, A., N.A. Rahman, and R. Yahya, *Moisture absorption effect on thermal, dynamic mechanical and mechanical properties of injection-molded short glass-fiber/polyamide 6,6 composites.* Fibers and Polymers, 2012. **13**(7): p. 899-906.

47. Pramoda, K.P. and T. Liu, *Effect of moisture on the dynamic mechanical relaxation of polyamide-6/clay nanocomposites.* Journal of Polymer Science Part B: Polymer Physics, 2004. **42**(10): p. 1823-1830.

48. Clark, R.L., M.D. Craven, and R.G. Kander, *Nylon 66/poly(vinyl pyrrolidone) reinforced composites: 2.* Composites Part A: Applied Science and Manufacturing, 1999. **30**(1): p. 37-48.

49. Akbar, S. and T. Zhang, *Moisture Diffusion in Carbon/Epoxy Composite and the Effect of Cyclic Hygrothermal Fluctuations: Characterization by Dynamic Mechanical Analysis (DMA) and Interlaminar Shear Strength (ILSS).* The Journal of Adhesion, 2008. **84**(7): p. 585-600.

50. Hu, H., et al., *Combined effect of relative humidity and temperature on dynamic viscoelastic properties and glass transition of poly(vinyl alcohol).* Journal of Applied Polymer Science, 2013. **130**(5): p. 3161-3167.

51. Nogueira, P., et al., *Effect of water sorption on the structure and mechanical properties of an epoxy resin system.* Journal of Applied Polymer Science, 2001. **80**(1): p. 71-80.

52. Parambath Mohan, R., *Investigation of Intra/ply Shear Behavior of Out-of-Autoclave Carbon/Epoxy Prepreg*. 2015, Concordia University.

53. Browning, C.J.C.e.p., *Processing science of graphite/epoxy composites.* chemical engineering progress, 1986. **82**(6): p. 41-44.

54. Costa, M.L., M.C. Rezende, and S.F.M. de Almeida, *Effect of Void Content on the Moisture Absorption in Polymeric Composites.* Polymer-Plastics Technology and Engineering, 2006. **45**(6): p. 691-698.

55. Hoa, S.V., *Principles of the manufacturing of composite materials*. 2009: DEStech Publications, Inc.

56. cycom® 5320-1 epoxy resin system technical data sheet. *(October 2015). Available: https://www.cytec.com/sites/default/files/datasheets/CYCOM%205320-1%20Rev%20CR5.pdf.*

57. Costa, M.L., S.F.M.d. Almeida, and M.C.J.M.R. Rezende, *Hygrothermal effects on dynamic mechanical snalysis and fracture behavior of polymeric composites.* Materials Research, 2005. **8**(3): p. 335-340.

58. Q800 Dynamic Mechanical Analyzer. Available: http://www.tainstruments.com/pdf/brochure/dma.pdf

59. A. Saha *et al*, "Study of jute fiber reinforced polyester composites by dynamic mechanical analysis," Journal of applied polymer science, vol. 71, pp. 1505-1513, 1999.

60. https://en.wikipedia.org/wiki/Dynamic_mechanical_analysis#cite_note-Nair-4 (2016/09/11).

61. Chawla, K.K. and M. Meyers, *Mechanical behavior of materials*. 1999: Cambridge university press.

62. Hancock, B.C. and G. Zografi, *The relationship between the glass transition temperature and the water content of amorphous pharmaceutical solids.* Pharmaceutical Research, 1994. **11**(4): p. 471-477.

63. Yang, B., et al., *Effects of moisture on the thermomechanical properties of a polyurethane shape memory polymer.* Polymer, 2006. **47**(4): p. 1348-1356.

64. Hojjati, M., et al., *Viscoelastic behavior of Cytec FM73 adhesive during cure.* Journal of Applied Polymer Science, 2004. **91**(4): p. 2548-2557.

65. Hinopoulos, G. and W.J.N.R.C. Broughton, *An improved modelling approach of moisture absorption in adhesive joints using the finite element method.* NPL Report CMMT (A), 1999. **204**.

66. Abaqus, C., *Analysis user's manual, Version 6.12*. 2012, ABAQUS.

67. Roe, N., et al., *Advanced moisture modeling of polymer composites.* Journal of Reinforced Plastics and Composites, 2013. **32**(7): p. 437-449.

68. Gibson, R.F., *Solutions Manual for Principles of Composite Material Mechanics*. 2007: CRC Press.

69. Shen, C.-H. and G.S. Springer, *Moisture Absorption and Desorption of Composite Materials.* Journal of Composite Materials, 2016. **10**(1): p. 2-20.